REFFERENCES

1 Kitagawa S., Kitaura R., Noro S.-I., Functional porous coordination polymers. **Angew. Chem. Int. Ed.** 2004; 43: 2334-2375.

2 Kitagawa S., Uemura K., Dynamic porous properties of coordination polymers inspired by hydrogen bonds. **Chem. Soc. Rev.** 2005; 34: 109-119.

3 Bailar J. C., Jr., **Preparative Inorganic Reaction.** 1964; 1.

4 Hoskins B. F., Robson R., Design and Construction of a New Class of Scaffolding-Like Materials Comprising Infinite Polymeric Frameworks of 3-D-Linked Molecular Rods. **J. Am. Chem. Soc.** 1990; 112: 1546-1554.

5 Kitagawa S., Kondo M., Formation of 1D and 3D Coordination Polymers in the Solid State Induced by Mechanochemical and Annealing Treatments: Bis(3-cyano-pentane-2,4-dionato) Metal Complexes. **Bull. Chem. Soc. Jpn.** 1998; 71: 1739-1753.

6 Moulton B., Zaworotko M. J., From molecules to crystal engineering: Supramolecular isomerism and polymorphism in network solids. **Chem. Rev.** 2001; 101: 1629-1658.

7 Khlobystov A. N., Blake A. J., Champness N. R., Lemenovskii D. A., Majouga A. G., Zyk N. V., Schroder M., Supramolecular design of one-dimensional coordination polymers based on silver(I) complexes of aromatic nitrogen-donor ligands. **Coord. Chem. Rev.** 2001; 222: 155-192.

8 Yaghi O. M., Keeffe M. O, Ockwig N. W., Chae H. K., Eddaoudi M., Kim J., Reticular synthesis and the design of new materials. **Nature.** 2003; 423: 705-714.

9 Rosi N. L., Eckert J., Eddaoudi M., Vodak D. Kim T., J., Keeffe M. O, Yaghi O. M., Hydrogen storage in microporous metal-organic frameworks. **Science.** 2003; 300: 1127-1129.

10 Dybtsev D. N., Chun H., Yoon S. H., Kim D., Kim K., Microporous manganese formate: A simple metal-organic porous material with high framework stability and highly selective gas sorption properties. **J. Am. Chem. Soc.** 2004; 126: 32-38.

11 Pan L., Adams K. M., Hernandez H. E., Wang X., Zheng C., Hattori Y., Kaneko K., Porous lanthanide-organic frameworks: Synthesis, characterization, and unprecedented gas adsorption properties. **J. Am. Chem. Soc.** 2003; 125: 3062-3067.

12 Zaworotko M. J., Superstructural diversity in two dimensions: crystal engineering of laminated solids. **Chem. Commun.** 2001; 1-9.

13 Banfi S., Carlucci L., Caruso E., Ciani G., Proserpio D. M., Using long bis(4-pyridyl) ligands designed for the self-assembly of coordination frameworks and architectures. **J. Chem. Soc. Dalton Trans.** 2002; 2714-2721.

14 Zhang H.-X., Kang B.-S., Xu A.-W., Chen Z.-N., Zhou Z.-Y., Chan A. S. C., Yu K.-B., Ren C., Supramolecular architectures from the self-assembly of trans-oxamidato-bridged dicopper(II) building blocks and phenyldicarboxylates. **J. Chem. Soc. Dalton Trans.** 2001; 2559-2566.

15 Prior T. J., Rosseinsky M. J., Crystal engineering of a 3-D coordination polymer from 2-D building blocks. **Chem. Commun.** 2001; 495-496.

16 Kumagai H., Kepert C. J., Kurmoo M., Construction of hydrogen-bonded and coordination-bonded networks of cobalt(II) with pyromellitate: Synthesis, structures, and magnetic properties. **Inorg. Chem.** 2002; 41: 3410-1422.

17 Chui S. S.-Y., Siu A., Feng X., Zhang Z. Y., Mak T. C. W., Williams I. D., Hydrothermal synthesis of three new 3-D framework rare-earth mellitates. **Inorg. Chem. Commun.** 2001; 4: 467-470.

18 Evans O. R., Lin W., Crystal engineering of NLO materials based on metal-organic coordination networks. **Acc. Chem. Res.** 2002; 35: 511-522.

19 Biradha K., Seward C., Zaworotko M. J. **Angew. Chem. Int. Ed.** 1999; 38: 492-495.

20 Okawa H., Ohba M., Structures and magnetism of cyanide-bridged bimetallic compounds: Design of complex-based magnetic materials. **Bull. Chem. Soc. Jpn.** 2002; 75: 1191-1203.

21 Noro S., Kitagawa S., Yamashita M., Wada T., Gavel 2-dimensional coordination polymer constructed from a multi-functional metalloligand. **CrystEngComm.** 2002; 4: 162-164.

22 Batten S. R., Hoskins B. F., Robson R., Two Interpenetrating 3D Networks Which Generate Spacious Sealed-Off Compartments Enclosing of the Order of 20 Solvent Molecules in the Structures of $Zn(CN)(NO_3)(tpt)_{2/3}$·solv (tpt = 2,4,6-tri(4-pyridyl)-1,3,5-triazine, solvent = $3/4C_2H_2Cl_4$·$3/4CH_3OH$ or $3/2CHCl_3$·$1/3CH_3OH$). **J. Am. Chem. Soc.** 1995; 117: 5385.

23 Chen B., Eddaoudi M., Hyde S. T., Keeffe M. O, Yaghi O. M., Interwoven metal-organic framework on a periodic minimal surface with extra-large pores. **Science.** 2001; 291: 1021-1023.

24 Kawata S., Kitagawa S., Kondo M., Furuchi I., Munakata M. **Angew. Chem.** 1994; 106: 1851–1854.

25 Kitagawa S., Kumagai H., Kudo C., Kamesaki H., Ishiyama T., Suzuki R., Kondo M., Katada M., Rational Design of a Novel Intercalation System. Layer-Gap Control of Crystalline Coordination Polymers, $\{[Cu(CA)(H_2O)_m](G)\}_n$ (m = 2, G = 2,5-Dimethylpyrazine and Phenazine; m = 1, G = 1,2,3,4,6,7,8,9-Octahydrophenazine). **Inorg. Chem.** 1996; 35: 4449-4461.

26 IUPAC Manual of Symbols and Terminology, Appendix 2, Pt.1. Colloid and Surface Chemistry. **Pure Appl. Chem.** 1972; 31: 578.

27 Brunauer S., Emmett P. H., Teller E., Adsorption of gases in multimolecular layers. **J. Am. Chem. Soc.** 1938; 60: 309-319.

28 Haynes J. M. , Functionalized poly(ether-anhydride) block copolymers, biodegradable polymers, composition including microspheres and nanospheres, and their use. **Mater. Struct.** 2006; 6: 1359-1360.

29 Brunauer S., Deming L. S., Deming W. E., Teller E., Chemisorptions of gases on iron synthetic-ammonia catalysts. **J. Am. Chem. Soc.** 1940; 62: 1723-1746.

30 Martin C., Tosi-Pellenq N., Patarin J., Coulomb J. P., Sorption Properties of AlPO4-5 and SAPO-5 Zeolite-like Materials. **Langmuir.** 1998; 14: 1774-1778.

31 Fletchera A. J., Thomasa K. M., Rosseinsky M. J., Flexibility in metal-organic framework materials: impact on sorption properties. **Solid State Chem J.** 2005; 178: 2491-2498.

32 Kondo M., Yoshitomi T., Seki K., Matsuzaka H., Kitagawa S., Asymmetric carbon-carbon bond formation promoted by divalent lanthanide complexes. **Angew. Chem.,** 1997; 109: 1844 – 1846.

33 Noro S., Kitaura R., Kondo M., Kitagawa S., Ishii T., Matsuzaka H., Yamashita M., Framework engineering by anions and porous functionalities of Cu(II)/4,4 '-bpy coordination polymers. **J. Am. Chem. Soc.** 2002; 124: 2568-2583.

34 Li D., Kaneko K., Molecular Geometry-Sensitive Filling in Semi-Rectangular Micropores of Organic-Inorganic Hybrid Crystals. **J. Phys. Chem. B.** 2000; 104: 8940-8945.

35 Eddaoudi M., Kim J., Rosi N., Vodak D., Wachter J., Keeffe M. O', Yaghi O. M., Systematic design of pore size and functionality in isoreticular MOFs and their application in methane storage. **Science**. 2002; 295: 469-474.

36 Jung O.-S., Kim Y. J., Lee Y.-A., Yoo K. H., Unique nanometer-thick layered network. **Chem. Lett.** 2002; 500-501.

37 Weitkamp J., Fritz M., Ernst S., Zeolites as media for hydrogen storage. **Int. J. Hydrogen Energy.** 1995; 20: 967-970.

38 Forster P. M., Eckert J., Chang J.-S., Park S.-E., FYrey G., Cheetham A. K., Hydrogen adsorption in nanoporous Nickel(II) phosphates. **J. Am. Chem. Soc.** 2003; 125: 1309-1312.

39 Yaghi O. M., Li H., T-Shaped Molecular Building Units in the Porous Structure of Ag(4,4'-bpy)·NO3. **J. Am. Chem. Soc.** 1996; 11: 295-296.

40 Min K. S., Suh M. P., Silver(I)-Polynitrile Network Solids for Anion Exchange: Anion-Induced Transformation of Supramolecular Structure in the Crystalline State. **J. Am. Chem. Soc.** 2000; 122: 6834-6840.

41 Fujita M., Kwon Y. J., Washizu S., Ogura K., Preparation, Clathration Ability, and Catalysis of a Two-Dimensional Square Network Material Composed of Cadmium(II) and 4,4'-Bipyridine. **J. Am. Chem. Soc.** 1994; 116: 1151-1152.

42 Tanski J. M., Wolczanski P. T., Covalent titanium aryldioxy one-, two-, and three-dimensional networks and their examination as Ziegler-Natta catalysts. **Inorg. Chem.** 2001; 40: 2026-2028.

43 Gomez-Lor B., GutiYrrez-Puebla E., Iglesias M., Monge M. Ruiz-Valero A., C., Snejko N., $In_2(OH)_3(BDC)_{1.5}$ (BDC=1,4-benzendicarboxylate): An In(III) supramolecular 3D framework with catalytic activity. **Inorg. Chem.** 2002; 41: 2429-2432.

44 Naito S., Tanibe T., Saito E., Miyao T., Mori W., A novel reaction pathway in olefln-deuterium exchange reaction inside the micropores of Rh(II) dicar boxylate polymer complexes. **Chem. Lett.** 2001; 1178-1179.

45 Xing B., Choi M.-F., Xu B., Design of coordination polymer gels as stable catalytic systems. **Chem. Eur. J.** 2002; 8: 5028-5032.

46 Seo J. S., Whang D., Lee H., Jun S. I., Oh J., Jeon Y. J., Kim K., A homochiral metal-organic porous material for enantioselective separation and catalysis. **Nature**. 2000; 404: 982-986.

47 Sawaki T., Aoyama Y., Immobilization of a Soluble Metal Complex in an Organic Network. Remarkable Catalytic Performance of a Porous Dialkoxy zirconium Polyphenoxide as a Functional Organic Zeolite Analogue. **J. Am. Chem. Soc.** 1999; 121: 4793--4798.

48 Evans O. R., Ngo H. L., Lin W., Chiral porous solids based on lamellar lantha-nide phosphonates. **J. Am. Chem. Soc.** 2001; 123: 10395-10396.

49 Pan L., Liu H., Lei X., Huang X., Olson D. H., Turro N. J., Li J. **Angew. Chem.** 2003; 115: 560 – 564.

50 Tannenbaum R., Three-Dimensional Coordination Polymers of Ruthenium(2+) with 1,4-Diisocyanobenzene Ligands and Their Catalytic Activity. **Chem. Mater.** 1994; 6: 550-555.

51 Tannenbaum R., Radiation enhancement of the catalytic properties of three-dimensional coordination polymers of Ru(II) with diisocyanide ligands. **J. Mol. Catal. A.** 1996; 107: 207-215.

52 Wu C.-D, Lin W., Photocatalytic properties of phosphor-doped titania nanoparticles. **Angew. Chem. Int. Ed.** 2007; 46: 1075.

53 Perles J., Iglesias M., Martın-Luengo M.-A, Monge M. A, Ruiz-Valero C., Snejko N., Metal-organic scandium framework: Useful material for hydrogen storage and catalysis. **Chem. Mater.** 2005; 17: 5837.

54 Schlichte K., Kratzke T., Kaskel S., Improved synthesis, thermal stability and catalytic properties of the metal-organic framework compound $CU_3(BTC)_2$. **Micro. Meso. Materials.** 2004; 73: 81-86.

55 Horike S., Dinca M., Tamaki K., Long J. R., Size-selective lewis acid catalysis in a microporous metal-organic framework with exposed Mn2+ coordination sites. **J. Am. Chem. Soc.** 2008; 130: 5854-5855

56 MacNicol D. D., McKendrick J. J., Wilson D. R., Clathrates and molecular inclusion phenomena. **Chem. Soc. Rev.** 1978; 7: 65-73.

57 Miyata M., Shibakami M., Chirachanchai S., Takemoto K., Kasai N. and Miki K., Guest-responsive structural changes in cholic acid intercalation crystals. **Nature.** 1990; 343: 446-447.

58 Kitaura R., Seki K., Akiyama G., Kitagawa S., Porous coordination-polymer crystals with gated channels specific for supercritical gases. **Angew. Chem., Int. Ed.** 2003; 42: 428-431.

59 Uemura K., Kitagawa S., Kondo M., Fukui K., Kitaura R., Chang H.-C., Mizutani T., Novel flexible frameworks of porous cobalt(III) coordination polymers that show selective guest adsorption based on the switching of hydrogen-bond pairs of amide groups. **Chem. Eur. J.** 2002; 8: 3586.

60 Muthu S., Yip J. H. K., Vittal J. J., Coordination networks of Ag(I) and N,N '-bis(3-pyridine-carboxamide)-1,6-hexane: structures and anion exchange. **J. Chem. Soc., Dalton Trans.** 2002; 4561-4568.

61 Biradha K., Hongo Y., Fujita M., Crystal-to-crystal sliding of 2D coordination layers triggered by guest exchange. **Angew. Chem. Int. Ed.** 2002; 41: 3395-3398.

62 Lu J. Y., Babb A. M., An extremely stable open-framework metal-organic polymer with expandable structure and selective adsorption capability. **Chem. Comm.** 2002; 1340-1341.

63 Matsuda R., Kitaura R., Kitagawa S., Kubota Y., Kobayashi T.C., Horike S., Takata M., Guest shape-responsive fitting of porous coordination polymer with shrinkable framework. **J. Am. Chem. Soc.** 2004; 126: 14063-14068.

64 Choi H.J., Suh M.P., Dynamic and redox active pillared bilayer open framework: Single-crystal-to-single-crystal transformations upon guest removal, guest exchange, and framework oxidation. **J. Am. Chem. Soc.** 2004; 126: 15844.

65 Ohmori O., Kawano M., Fujita M., Crystal-to-crystal guest exchange of large organic molecules within a 3D coordination network. **J. Am. Chem. Soc.** 2004; 126: 16292.

66 Uemura K., Kitagawa S., Fukui K., Saito K., A Contrivance for a Dynamic Porous Framework: Cooperative Guest Adsorption Based on Square Grids Connected by Amide-Amide Hydrogen Bonds. **J. Am. Chem. Soc.** 2004; 126: 3817-3821.

67 Youngme S., Cheansirisomboon A., Danvirutai C., Chaichit N., Pakawatchai C., van Albabda G.A., Reedijk J., Polynuclear paddle-wheel copper(II) propionate with di-2-pyridylamine or 1,10-phenanthroline: Preparation, characterization and X-ray structure. **Inorg. Chem. Commun.** 2008; 9: 57.

68 Luo J., Hong M. C, Wang R., Cao R., Han L., Yuan D., Lin Z., Zhou Y., A novel bilayer cobalt(II)-Organic framework with nanoscale channels accommodating large organic molecules. **Inorg. Chem.** 2003; 42: 4486.

69 Suh M. P., Ko J. W., Choi H. J., A metal-organic bilayer open framework with a dynamic component: Single-crystal-to-single-crystal transformations. **J. Am. Chem. Soc.** 2002; 124: 10976.

70 Phuengphai P., Youngme S., Kongsaeree P., Pakawatchai C., Chaichit N., Teat S.J., Gamez P., Reedijk J., Drastic steric effects from, respectively, a hydrogen, a methyl and an ethyl group on the coordination network of a zinc(II)-4,4'-bipyridine-carboxylato ternary system. **CrystEngComm.** 2009; 11: 1723.

71 Phuengphai P., Youngme S., Gamez P., Reedijk J., Catalytic properties of a series of coordination networks: cyanosilylation of aldehydes catalyzed by Zn(II)-4,4'-bpy-carboxylato complexes. **Dalton Trans.** 2010; accepted.

72 Shi W. J., Ruan C. X., Li Z., Li M., Li D., Tuning framework formation by flexible ligand elongation and second ligating spacer variation: increasing dimensionality and macrocycle size. **CrystEngComm.** 2008; 10: 778.

73 Brammer L., Developments in inorganic crystal engineering. **Chem. Soc. Rev.** 2004; 33: 476-489.

74 Choi H. J., Suh M. P., Dynamic and redox active pillared bilayer open framework: Single-crystal-to-single-crystal transformations upon guest removal, guest exchange, and framework oxidation. **J. Am. Chem. Soc.** 2004; 126: 15844-15851.

75 Albrecht M., Lutz M., Spek A. L., van Koten G., Organoplatinum crystals for gas-triggered switches. **Nature.** 2000; 406: 970-974.

76 Valli V. L. K., Alper H., Reductive carbonylation of mono- and dinitroarenes catalyzed by montmorillonitebipyridinylpalladium(II) acetate and ruthenium carbonyl. **J. Am. Chem. Soc.** 1993; 115: 3778-3779.

90 Evans O. R., Ngo H. L., Lin W. B., Chiral porous solids based on lamellar lanthanide phosphonates. **J. Am. Chem. Soc.** 2001; 123: 10395-10396.

77 Noro S.-I., Kitaura R., Kondo M., Kitagawa S., Ishii T., Matsuzaka H., Yamashita M., Framework engineering by anions and porous functionalities of Cu(II)/4,4 '-bpy coordination polymers. **J. Am. Chem. Soc.** 2002; 124: 2568.

78 Jung O-S., Kim Y. J., Lee Y. A., Park J. K., Chae H. K., Smart Molecular Helical Springs as Tunable Receptors. **J. Am. Chem. Soc.** 2000; 122: 9921-9925.

79 SAINT. **Software Reference Manual. Siemens Analytical X-Ray Systems Version 4**. Madison: WI; 1996.

80 Sheldrick G. M., SADABS. **Program for Empirical Absorption correction of Area Dectector**. Germany: University of Gőttingen; 1997.

81 SHELXTL. **Reference Manual. 1997; Siemens Analytical X-Ray Systems Version 6.12.** Madison: WI; 1996.

82 Dai Y. M., Ma E., Tang E., Zhang J., Li Z. J., Huang X. D., Yao Y. G., Paratactic assembly of two distinct units into a unique 3D architecture. **Cryst. Growth Des.** 2005; 5: 1313-1315.

83 Miao X. H., Xiao H. P., Zhu L. G., Poly[zinc(II)-mu(2)-4,4 '-bipyridine-di-mu(2)-formato]: a chiral three-dimensional coordination polymer. **Acta Crystallogr. E.** 2006; 62: M1756-M1757.

84 Woodward J. D., Backov R. V., Abboud K. A., Talham D. R., Monomers, chains, ladders, and two-dimensional sheets: Structural diversity in six new compounds of Zn(II) with 4,4 '-bipyridine. **Polyhedron.** 2006; 25: 2605-2615.

85 Zheng Y. Z., Tong M. L., Chen X. M., Syntheses, structures and magnetic properties of five coordination polymers derived via in situ metal-ligand reactions of 2-phenyl-malonic acid. **J. Mol. Struct.** 2006; 796: 9-17.

86 Conerney B., Jensen P., Kruger P. E., Moubaraki B., Murray K. S., Synthesis and structural characterisation of two coordination polymers (molecular ladders) incorporating $[M(OAc)_2]_2$ secondary building units and 4,4 '-bipyridine [M = Cu(II), Zn(II)]. **CrystEngComm.** 2003; 5: 454-458.

87 Lee T. W., Lau J. P. K., Wong W. T., Synthesis and characterization of coordination polymers of Zn(II) with 1,3-bis(4-pyridyl)propane and 4,4'-pyridine ligands. **Polyhedron**. 2004; 23: 999-1002.

88 Ma D. Y., Deng G. H., A novel one-dimensional zinc coordination polymer containing 4-methylbenzoate and 4,4-bipyridine. **Acta Crystallogr. C.** 2008; 64: M271-M273.

89 Wang C. F., Zhu Z. Y., Zhang Z. X., Chen Z. X., X. G. Zhou, Crystal engineering of zinc(II) and copper(II) complexes containing 3,5-dimethyl isoxazole-4-carboxylate ligand via O-H center dot center dot center dot N, C-H center dot center dot center dot A (A = N, O and pi) and bifurcated C-H center dot center dot center dot N/O interactions. **CrystEngComm.** 2007; 9: 35-38.

90 Ghedini M., Deda M. L., Aiello I., Grisolia A., Synthesis and photophysical characterisation of luminescent zinc complexes with 5-substituted-8-hydroxyquinolines. **J. Chem. Soc., Dalton Trans.** 2002; 3406-3409.

91 Hathaway B. J., Wilkinson G., Gill R. D., McCleverty J. A., **Comprehensive Coordination Chemistry.** 1987; (Eds.) 5: Pergamon Press, Oxford.

92 Nakamoto K., **Infrared and Raman spectra of inorganic and coordination compounds.** John Wiley & Sons, New York, 1997.

93 Ohmori O., Fujita M., Heterogeneous catalysis of a coordination network: cyanosilylation of imines catalyzed by a Cd(II)-(4,4'-bipyridine) square grid complex. **Chem. Commun.** 2004; 1586-1587.

94 Biradha K., Crystal engineering: from weak hydrogen bonds to co-ordination bonds. **CrystEngComm.** 2003; 5: 374-384.

95 Almeida Paz F.A., Bond A. D., Khimyak Y. Z., Klinowski J., Synthesis and characterization of a new layered compound of trimesic acid. **New J. Chem.** 2002; 26: 381-383.

96 Aakeroy C. B., Beffert K., Desper J., Elisabeth E., Hydrogen-bond directed structural selectivity in asymmetric heterocyclic cations. **Cryst. Growth Des.** 2003; 3: 837-846.

97 Cui Y., Ngo H. L., White P. S., Lin W., Hierarchical assembly of homochiral porous solids using coordination and hydrogen bonds. **Inorg. Chem.** 2003; 42: 652-660.

98 Vilar R., Anion-templated synthesis. **Angew. Chem. Int. Ed.** 2003; 42: 1460.

99 Biradha K., Sarkar M., Rajput L., Crystal engineering of coordination polymers using 4,4 '-bipyridine as a bond between transition metal atoms. **Chem. Commun.** 2006; 4169-4179.

100 Otwinowski Z., Minor W., Processing of x-ray diffraction data collected in oscillation mode. **Macromol. Crystallogr.** A. 1997; 276: 307–326.

101 Altomare A., Cascarano G., Giacovazzo C., Guagliardi A., Burla M. C., Polidori G., Camalli M., **J. Appl. Crystallogr.** 1994; 27: 435.

102 SHELX-TL; Bruker AXS: Madison, WI, 2001.

103 Youngme S., Chaichit N., Damnatara K., The coordination chemistry of dinitrato-di-2-pyridylamine copper(II). Crystal structures of catena-poly[[(di-2-pyridylamine)(nitrato-O,O ')copper(II)]-mu-nitrato-O : O '] and bis(nitrato-O,O')(di-2-pyridylamine)copper(II) dihydrate. **Polyhedron.** 2002; 21: 943-950.

104 Gotz R.J, Robertazzi A., Mutikainen I., Turpeinen U, Gamez P., Reedijk J., Concurrent anion center dot center dot center dot pi interactions between a perchlorate ion and two pi-acidic aromatic rings, namely pentafluorophenol and 1,3,5-triazine. **Chem. Commun.** 2008; 3384–3386.

105 Youngme S., Phuengphai P., Pakawatchai C., van Albada G.A., Reedijk J.,A novel polymeric trinuclear-based mu(3)-phosphato-bridged Cu(II) complex containing two different types of monophosphate. Synthesis, structure and magnetism of $\{[Cu_3(di\text{-}2\text{-}puridylamine)_3(mu_3),eta_3\text{-}HPO_4)(mu_3),eta_4\text{-}PO_4)(H_2O)](PF_6)(H_2O)_3\}_n$. **Inorg. Chim. Acta.** 2005; 358: 2125-2128.

106 Manson J. L., Lecher J. G., Gu J., Geiser U., Schlueter J. A., Henning R., Wang X., Schultz A. J., Koo H.-J., Whangbo M.-H., $Cu(HCO_2)_2L$ {L = pyrazine, 4,4'-bipyridine}: employing the formate anion as a building block in three-dimen sional coordination polymers. **J. Chem. Soc. Daton Trans.** 2003; 2905–2911.

107 Zhu L.-G., Kitagawa S., A 2-D polymer constructed through bridging acetate, hydroxo, aqua and bipyridine ligands: crystal structure of $\{[Cu_2(mu\text{-}CH_3COO)(mu\text{-}OH)(mu\text{-}H_2O)(4,4'\text{-}bipy)]2H_2O)(SiF_6)\}_n$. **Inorg. Chem. Commun.** 2002; 5: 358–360.

108 Yang E., Wang X.-Q., Qin Y.-Y., A novel 3D supramolecular network constructed from $[Cu(4,4\text{-}bipyridine)(O_2CMe)_2]_2$ molecular ladders by hydrogen Bonding. **Chinese J. Struct. Chem.** 2006; 25: 1365-1368.

109 Biswas J. D., Masuda, Mitra S., Mechanism of HMGB1 release inhibition from RAW264.7 cells by oleanolic acid in Prunus mume Sieb. et Zucc.. **Struct. Chem.** 2007; 18: 9–13.

110 Castineiras A., Balboa S., Bermejo E., Anorg Z., Weak antiferromagnetism in carboxylato copper(II) complexes of bipyridines. **Allg. Chem.** 2002; 628: 1116-1123.

110 Wen Y.-H., He Y.-H., Feng Y.-L., Ng S. W., Crystal structure of catena-[(tetrakis-mu(2)-acetato-mu(2)-4,4'-bipyridine) dicopper(II)]acetonitrile solvate. **Chinese J. Struct. Chem.** 2007; 26: 29-32.

111 Bie H.-Y., Yu J.-H., Zhao K., Lu J., Duan L.-M., Xu J.-Q., Syntheses, characterization and fluorescent properties of two square pyramidal Cu (II) inorganic-organic hybrid polymers. **J. Mol. Struct.** 2005; 741: 77–84.

112 Wang C. F., Zhu Z. Y., Zhang Z. X., Chen Z. X., Zhou X. G., Crystal engineering of zinc(II) and copper(II) complexes containing 3,5-dimethylisoxazole-4-carboxylate ligand via O-H center dot center dot center dot N, C-H center dot center dot center dot A (A = N, O and pi) and bifurcated C-H center dot center dot center dot N/O interactions. **CrystEngComm.** 2007; 9: 35-38.

113 Zhu L.-G., Kitagawa S., Miyasaka H., Chang H.-C., Syntheses and crystal structures of three one-dimensional copper(II) complexes constructed by salicylate and 4,4 '-bipyridine: ladder, zig-zag, and linear polymeric assembly. **Inorg. Chim. Acta.** 2003; 355: 121-126.

114 Hathaway B.J., Wilkinson G., Gill R.D., McCleverty J.A. (Eds.), **Comprehensive Coordination Chemistry.** Pergamon Press, Oxford. 1987: 5.

115 Somanathan R., Rivero I.A., Gama A., Ochoa A., Aguirre G., **Synth. Commun.** 1998; 28: 2043.

116 Moulton B., Zaworotko M.J., From molecules to crystal engineering: Supramolecular isomerism and polymorphism in network solids. **Chem. Rev.** 2001; 101: 1629.

117 Uemura T., Hoshino Y., Kitagawa S., Yoshida K., Isoda S., Effect of organic polymer additive on crystallization of porous coordination polymer. **Chem. Mater.** 2006; 18: 992.

118 Shimomura S., Matsuda R., Tsujino T., Kawamura T., Kitagawa S., TCNQ dianion-based coordination polymer whose open framework shows charge-transfer type guest inclusion. **J. Am. Chem. Soc.** 2006; 128: 16416.

APPENDICES

APPENDIX A

Supplementary Data for X-ray powder diffraction patterns of zinc(II)-4,4'-bpy-carboxylato compounds (1, 2 and 4-11) and copper(II)-4,4'-bpy-carboxylato compounds 12, 14, 16 and 18

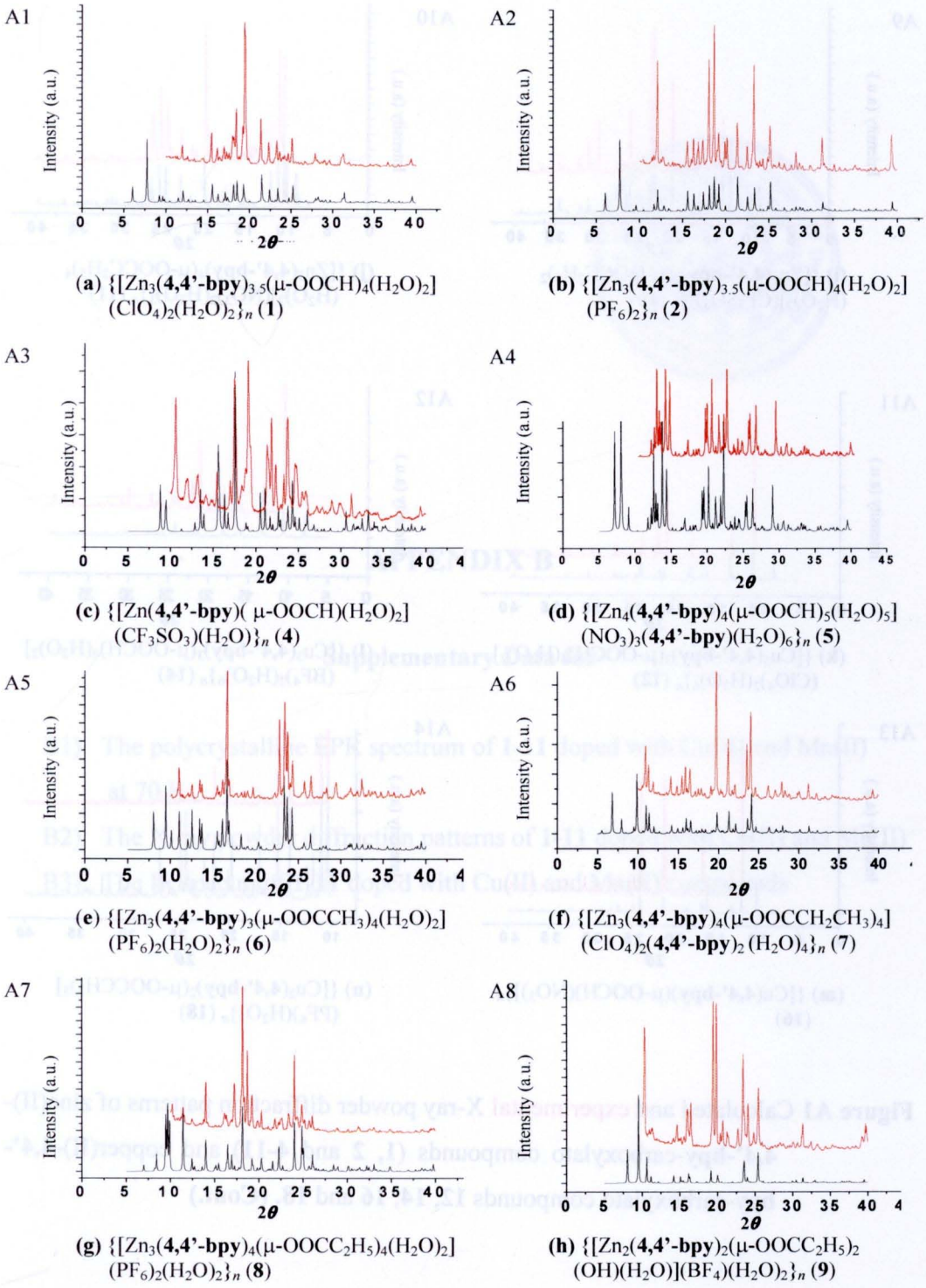

(a) {[Zn_3(**4,4'-bpy**)$_{3.5}$(μ-OOCH)$_4$(H_2O)$_2$] (ClO_4)$_2$(H_2O)$_2$}$_n$ (**1**)

(b) {[Zn_3(**4,4'-bpy**)$_{3.5}$(μ-OOCH)$_4$(H_2O)$_2$] (PF_6)$_2$}$_n$ (**2**)

(c) {[Zn(**4,4'-bpy**)(μ-OOCH)(H_2O)$_2$] (CF_3SO_3)(H_2O)}$_n$ (**4**)

(d) {[Zn_4(**4,4'-bpy**)$_4$(μ-OOCH)$_5$(H_2O)$_5$] (NO_3)$_3$(**4,4'-bpy**)(H_2O)$_6$}$_n$ (**5**)

(e) {[Zn_3(**4,4'-bpy**)$_3$(μ-$OOCCH_3$)$_4$(H_2O)$_2$] (PF_6)$_2$(H_2O)$_2$}$_n$ (**6**)

(f) {[Zn_3(**4,4'-bpy**)$_4$(μ-$OOCCH_2CH_3$)$_4$] (ClO_4)$_2$(**4,4'-bpy**)$_2$ (H_2O)$_4$}$_n$ (**7**)

(g) {[Zn_3(**4,4'-bpy**)$_4$(μ-$OOCC_2H_5$)$_4$(H_2O)$_2$] (PF_6)$_2$(H_2O)$_2$}$_n$ (**8**)

(h) {[Zn_2(**4,4'-bpy**)$_2$(μ-$OOCC_2H_5$)$_2$ (OH)(H_2O)][BF_4)(H_2O)$_2$}$_n$ (**9**)

Figure A1 Calculated and experimental X-ray powder diffraction patterns of zinc(II)-**4,4'-bpy**-carboxylato compounds (**1**, **2** and **4-11**) and copper(II)-**4,4'-bpy**-carboxylato compounds **12**, **14**, **16** and **18.**

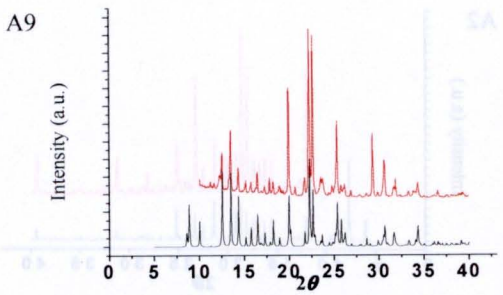

(i) $\{[Zn_2(\mathbf{4,4'\text{-}bpy})_2(\mu\text{-}OOCC_2H_5)_2(H_2O)_2](CF_3SO_3)_2\}_n$ (**10**)

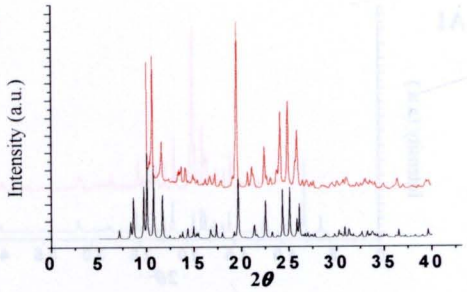

(j) $\{[Zn_3(\mathbf{4,4'\text{-}bpy})_4(\mu\text{-}OOCC_2H_5)_4(H_2O)_2](NO_3)_2(H_2O)_3\}_n$ (**11**)

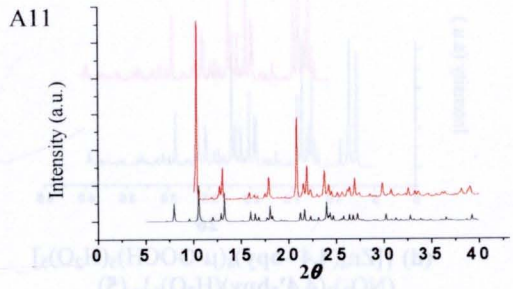

(k) $\{[Cu_3(\mathbf{4,4'\text{-}bpy})_3(\mu\text{-}OOCH)_4(H_2O)_2](ClO_4)_2(H_2O)_6\}_n$ (**12**)

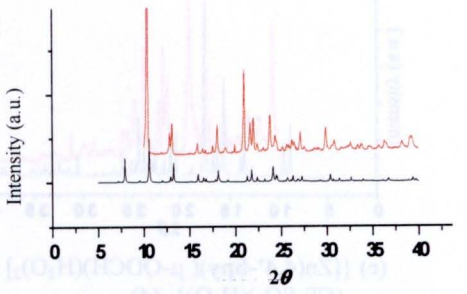

(l) $\{[Cu_3(\mathbf{4,4'\text{-}bpy})_3(\mu\text{-}OOCH)_4(H_2O)_2](BF_4)_2(H_2O)_6\}_n$ (**14**)

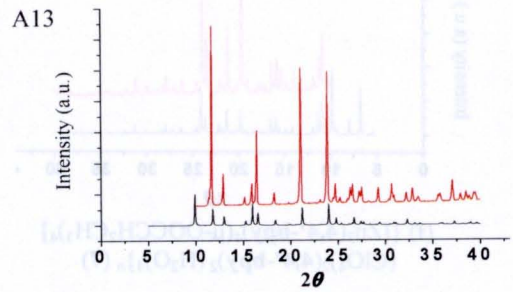

(m) $\{[Cu(\mathbf{4,4'\text{-}bpy})(\mu\text{-}OOCH)(NO_3)]\}_n$ (**16**)

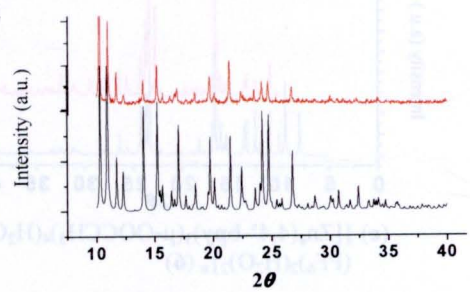

(n) $\{[Cu_2(\mathbf{4,4'\text{-}bpy})_2(\mu\text{-}OOCCH_3)_3](PF_6)(H_2O)\}_n$ (**18**)

Figure A1 Calculated and experimental X-ray powder diffraction patterns of zinc(II)-**4,4'-bpy**-carboxylato compounds (**1**, **2** and **4-11**) and copper(II)-**4,4'-bpy**-carboxylato compounds **12**, **14**, **16** and **18. (Cont.)**

APPENDIX B

Supplementary Data for

B1) The polycrystalline EPR spectrum of **1-11** doped with Cu(II) and Mn(II) at 70 K

B2) The X-ray powder diffraction patterns of **1-11** doped with Cu(II) and Mn(II)

B3) The IR spectra of **1-11** doped with Cu(II) and Mn(II) compounds

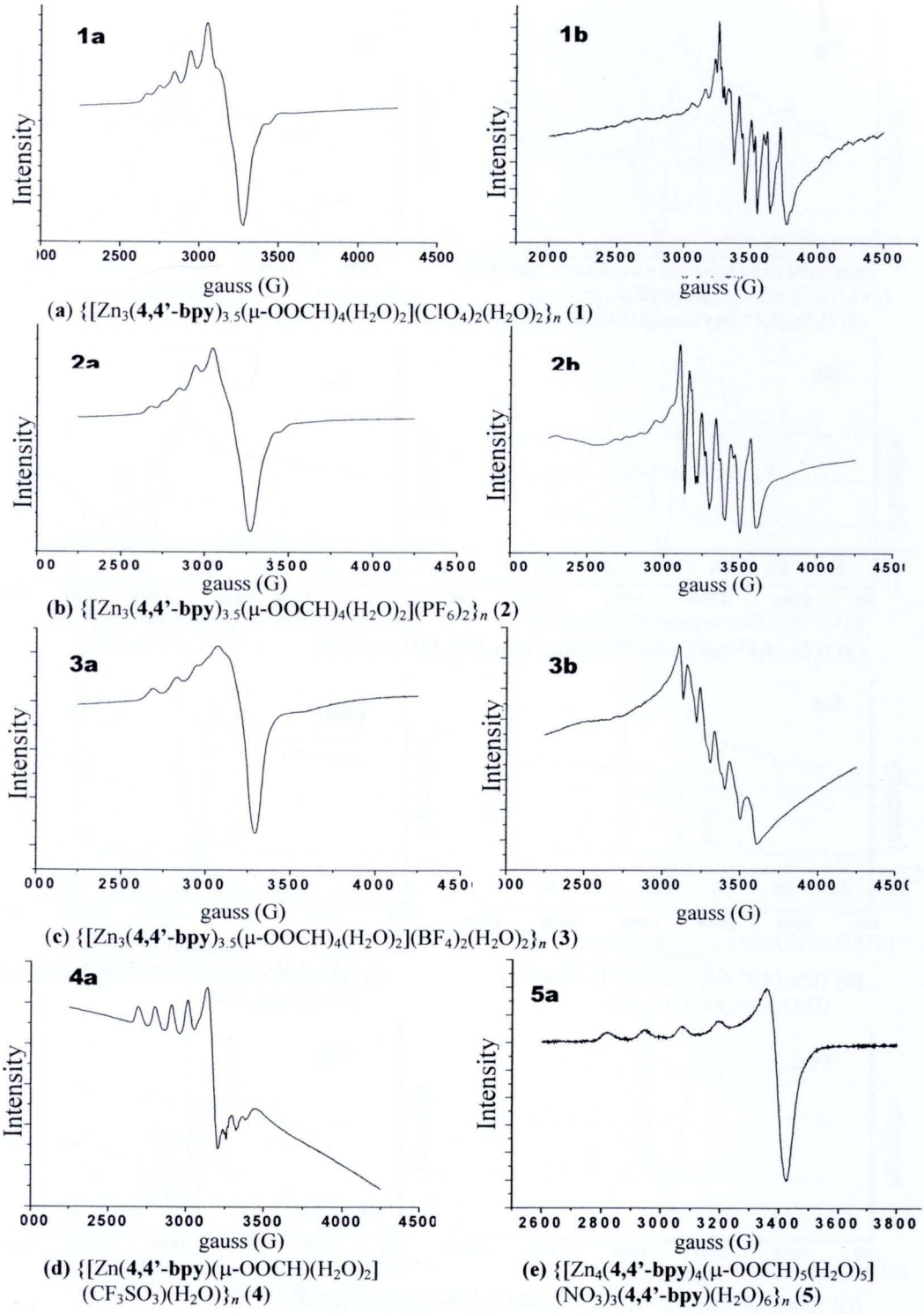

(a) $\{[Zn_3(\mathbf{4,4'\text{-}bpy})_{3.5}(\mu\text{-}OOCH)_4(H_2O)_2](ClO_4)_2(H_2O)_2\}_n$ (**1**)

(b) $\{[Zn_3(\mathbf{4,4'\text{-}bpy})_{3.5}(\mu\text{-}OOCH)_4(H_2O)_2](PF_6)_2\}_n$ (**2**)

(c) $\{[Zn_3(\mathbf{4,4'\text{-}bpy})_{3.5}(\mu\text{-}OOCH)_4(H_2O)_2](BF_4)_2(H_2O)_2\}_n$ (**3**)

(d) $\{[Zn(\mathbf{4,4'\text{-}bpy})(\mu\text{-}OOCH)(H_2O)_2](CF_3SO_3)(H_2O)\}_n$ (**4**)

(e) $\{[Zn_4(\mathbf{4,4'\text{-}bpy})_4(\mu\text{-}OOCH)_5(H_2O)_5](NO_3)_3(\mathbf{4,4'\text{-}bpy})(H_2O)_6\}_n$ (**5**)

Figure B1 The polycrystalline EPR spectra of **1-5** and **7-11**

(a) doped with Cu(II) at 70 K

(b) doped with Mn(II) at 70 K.

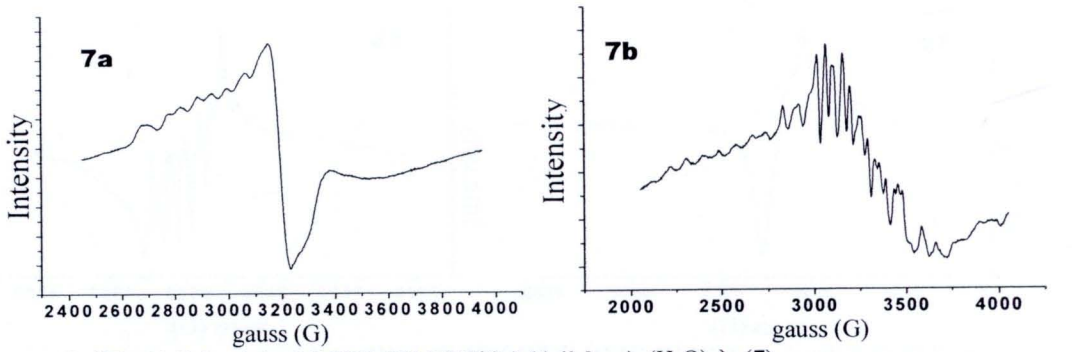

(f) $\{[Zn_3(\mathbf{4,4'\text{-}bpy})_4(\mu\text{-}OOCCH_2CH_3)_4](ClO_4)_2(\mathbf{4,4'\text{-}bpy})_2(H_2O)_4\}_n$ (7)

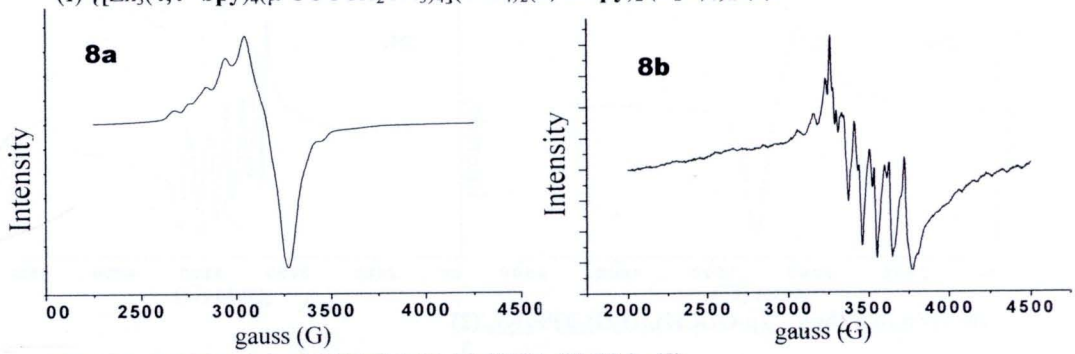

(g) $\{[Zn_3(\mathbf{4,4'\text{-}bpy})_4(\mu\text{-}OOCC_2H_5)_4(H_2O)_2](PF_6)_2(H_2O)_2\}_n$ (8)

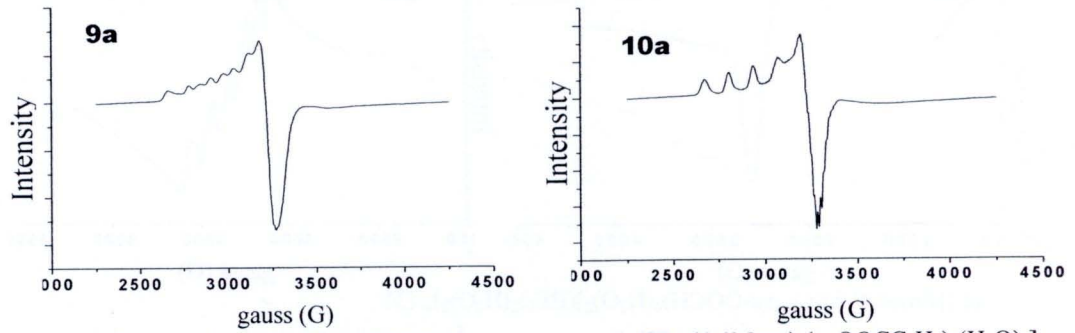

(h) $\{[Zn_2(\mathbf{4,4'\text{-}bpy})_2(\mu\text{-}OOCC_2H_5)_2(OH)(H_2O)](BF_4)(H_2O)_2\}_n$ (9)

(i) $\{[Zn_2(\mathbf{4,4'\text{-}bpy})_2(\mu\text{-}OOCC_2H_5)_2(H_2O)_2](CF_3SO_3)_2\}_n$ (10)

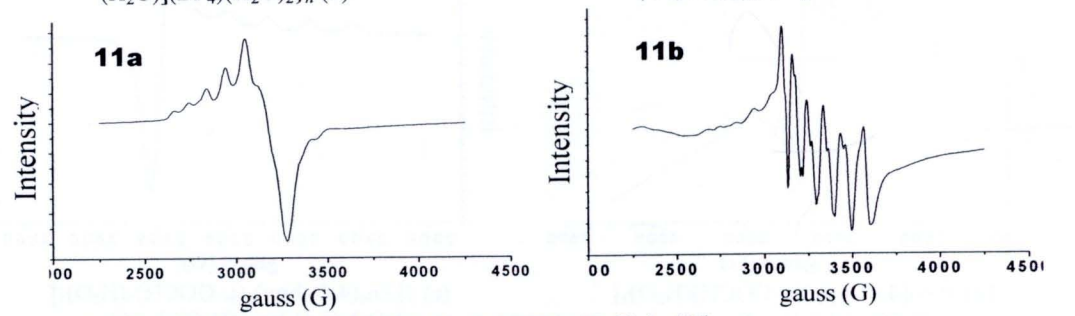

((j) $\{[Zn_3(\mathbf{4,4'\text{-}bpy})_4(\mu\text{-}OOCC_2H_5)_4(H_2O)_2](NO_3)_2(H_2O)_3\}_n$ (11)

Figure B1 The polycrystalline EPR spectra of **1-5** and **7-11**

(a) doped with Cu(II) at 70 K

(b) doped with Mn(II) at 70 K. **(Cont.)**

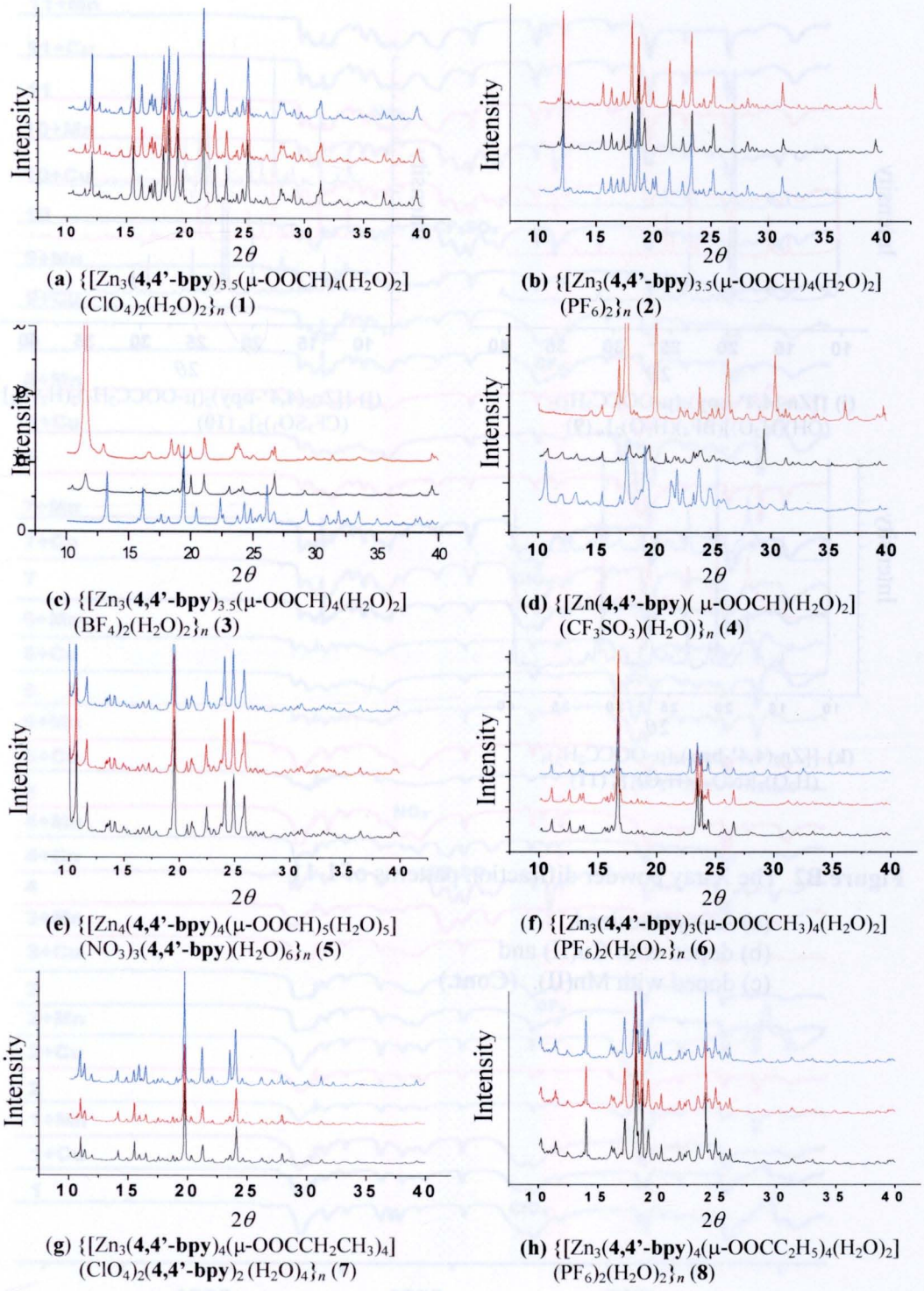

(a) $\{[Zn_3(\mathbf{4,4'\text{-}bpy})_{3.5}(\mu\text{-}OOCH)_4(H_2O)_2](ClO_4)_2(H_2O)_2\}_n$ (**1**)

(b) $\{[Zn_3(\mathbf{4,4'\text{-}bpy})_{3.5}(\mu\text{-}OOCH)_4(H_2O)_2](PF_6)_2\}_n$ (**2**)

(c) $\{[Zn_3(\mathbf{4,4'\text{-}bpy})_{3.5}(\mu\text{-}OOCH)_4(H_2O)_2](BF_4)_2(H_2O)_2\}_n$ (**3**)

(d) $\{[Zn(\mathbf{4,4'\text{-}bpy})(\mu\text{-}OOCH)(H_2O)_2](CF_3SO_3)(H_2O)\}_n$ (**4**)

(e) $\{[Zn_4(\mathbf{4,4'\text{-}bpy})_4(\mu\text{-}OOCH)_5(H_2O)_5](NO_3)_3(\mathbf{4,4'\text{-}bpy})(H_2O)_6\}_n$ (**5**)

(f) $\{[Zn_3(\mathbf{4,4'\text{-}bpy})_3(\mu\text{-}OOCCH_3)_4(H_2O)_2](PF_6)_2(H_2O)_2\}_n$ (**6**)

(g) $\{[Zn_3(\mathbf{4,4'\text{-}bpy})_4(\mu\text{-}OOCCH_2CH_3)_4](ClO_4)_2(\mathbf{4,4'\text{-}bpy})_2(H_2O)_4\}_n$ (**7**)

(h) $\{[Zn_3(\mathbf{4,4'\text{-}bpy})_4(\mu\text{-}OOCC_2H_5)_4(H_2O)_2](PF_6)_2(H_2O)_2\}_n$ (**8**)

Figure B2 The X-ray powder diffraction patterns of **1-11**

(a) As-synthesized,
(b) doped with Cu(II) and
(c) doped with Mn(II).

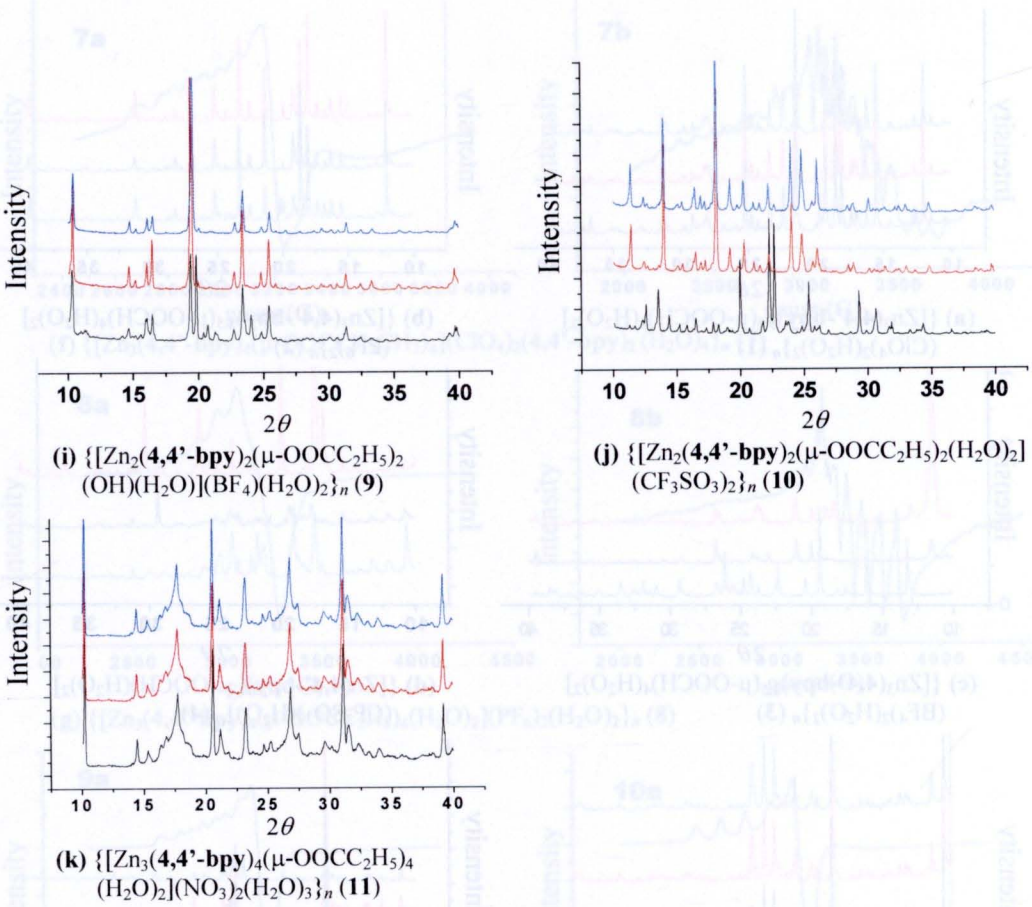

Figure B2 The X-ray powder diffraction patterns of **1-11**

(a) As-synthesized,
(b) doped with Cu(II) and
(c) doped with Mn(II). **(Cont.)**

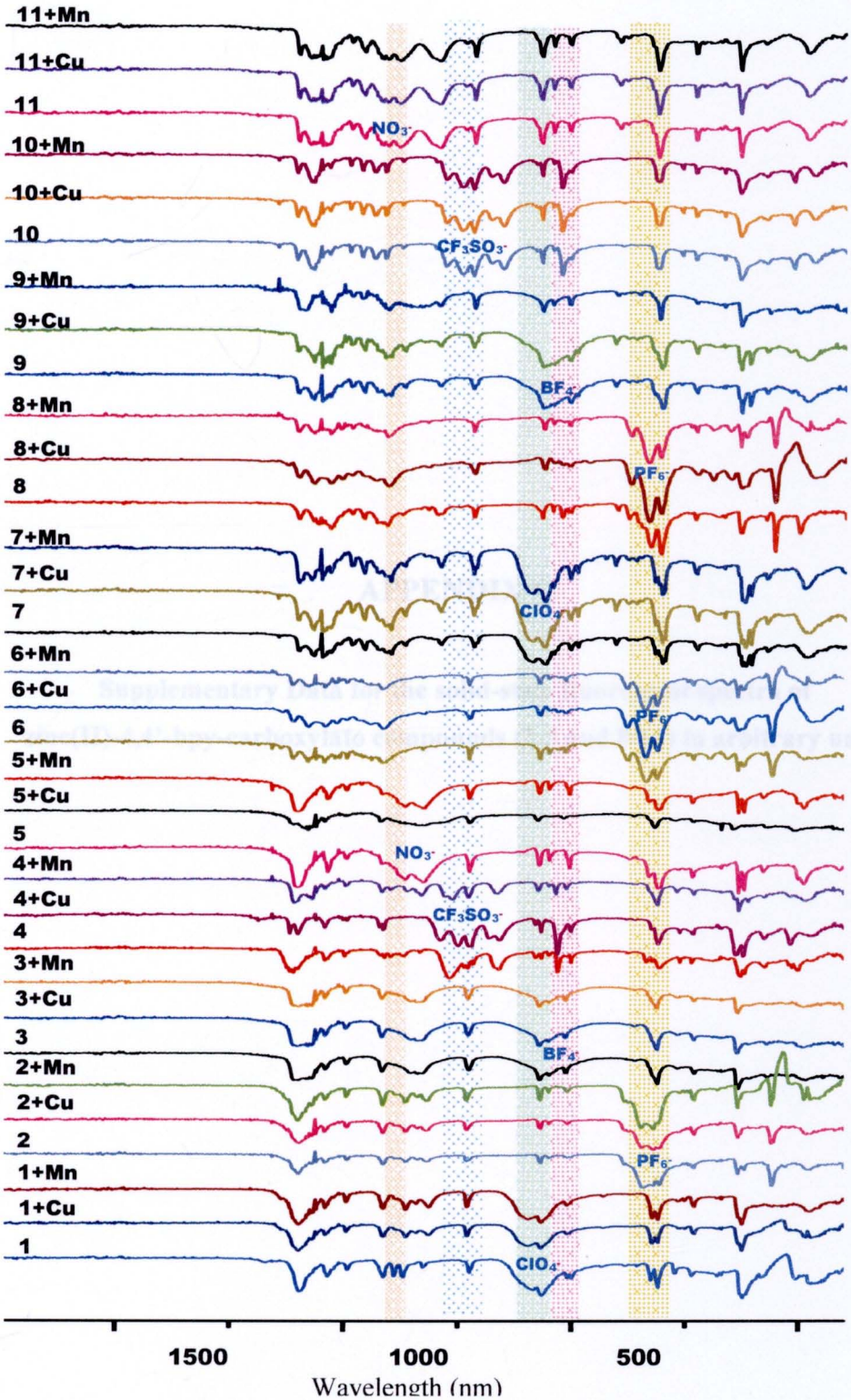

Figure B3 IR spectra of **1-11** doped with Cu(II) and Mn(II).

APPENDIX C

Supplementary Data for the solid-state fluorescent spectra of zinc(II)-4,4'-bpy-carboxylato compounds (2-5 and 8-11) in arbitrary units

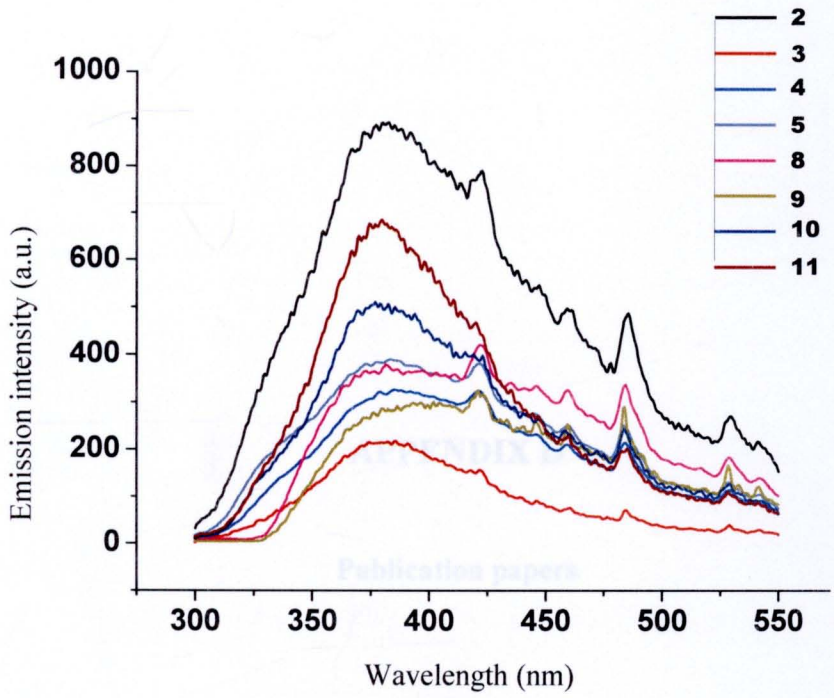

Figure C1 The solid-state fluorescent spectra of zinc(II)-**4,4'-bpy**-carboxylato compounds (**2-5** and **8-11**) in arbitrary units

2
3
4
5
6
9
10
11
1000
800
600
400
200
0
Emission Intensity (a.u.)
300
350
400
450
500
550
Wavelength (nm)

APPENDIX D

Publication papers

PAPER www.rsc.org/crystengcomm | CrystEngComm

Drastic steric effects from, respectively, a hydrogen, a methyl and an ethyl group on the coordination network of a zinc(II)–4,4′-bipyridine–carboxylato ternary system†

Pongthipun Phuengphai,[a] Sujittra Youngme,*[a] Palangpon Kongsaeree,[b] Chaveng Pakawatchai,[c] Narongsak Chaichit,[d] Simon J. Teat,[e] Patrick Gamez[f] and Jan Reedijk[f]

Received 26th January 2009, Accepted 5th May 2009
First published as an Advance Article on the web 21st May 2009
DOI: 10.1039/b901607d

The combination of a [zinc(II)–**4,4′-bpy**] coordination moiety with, respectively, formato, acetato and propionato ligands leads to the formation of the compounds $\{[Zn_3(4,4'\text{-bpy})_{3.5}(\mu\text{-}O_2CH)_4(H_2O)_2](ClO_4)_2(H_2O)_2\}_n$ (**1**), $\{[Zn_3(4,4'\text{-bpy})_3(\mu\text{-}O_2CCH_3)_4(H_2O)_2](PF_6)_2(H_2O)_2\}_n$ (**2**) and $\{[Zn_3(4,4'\text{-bpy})_4(\mu\text{-}O_2CCH_2CH_3)_4](ClO_4)_2(4,4'\text{-bpy})_2(H_2O)_4\}_n$ (**3**). The molecular structures determined by single-crystal X-ray diffraction data reveal significant changes, which are apparently due to the sole different steric hindrance between a H atom (formato, compound **1**), a methyl group (acetato, compound **2**) and an ethyl group (propionato, compound **3**). The three coordination materials have been fully characterized and their thermal decomposition behavior has been investigated. The 3D (**1**), 1D (**2**) and 2D (**3**) networks exhibit voids that contain the counter-ions and guest molecules as well, namely water for compounds **1** and **2**, and water/**4,4′-bpy** for compound **3**.

Introduction

During the past 15 years, the field of coordination polymer research has become an extremely prolific area of chemistry.[1–3] In this context, a number of crystal engineering investigations are aimed at trying to understand how a variety of factors, like the metal ions, reaction conditions and secondary co-ligands,[4] may affect the molecular structures and/or properties of coordination polymers.[5–7]

Coordination polymer networks, also known as metal–organic frameworks (MOFs),[8] are based upon self-assembly between metal ions (typically transition-metal ions) characterized by inherent preferences in coordination geometry and at least dinucleating ligands.[9] (Poly)carboxylato ligands are commonly being used to generate MOFs of diverse topologies.[10] Moreover, the combination of metal-carboxylato building blocks with a secondary co-ligand (usually a dinucleating N-donor ligand, such as 4,4′-bipyridine, **4,4′-bpy**) allows a considerable enhancement of the structural diversity of the coordination materials.[11] Actually, numerous remarkable coordination networks built from **4,4′-bpy** and carboxylato ligands have been reported in the literature,[12–19] for which the nature of the carboxylato molecule plays an important structural role.[20–23]

In the present study, the effect of the steric hindrance of different carboxylato ligands (formato, acetato and propionato ligands) on the solid-state structure of the corresponding coordination materials has been investigated. Thus, three multicomponent polymeric networks have been synthesized from zinc(II) ions, **4,4′-bpy** and a carboxylato ligand, whose single-crystal X-ray structures reveal a significant influence of a hydrogen (formate), a methyl (acetate) and an ethyl (propionate) group on the assembly of the coordination framework. The compounds $\{[Zn_3(4,4'\text{-bpy})_{3.5}(\mu\text{-}O_2CH)_4(H_2O)_2](ClO_4)_2(H_2O)_2\}_n$ (**1**), $\{[Zn_3(4,4'\text{-bpy})_3(\mu\text{-}O_2CCH_3)_4(H_2O)_2](PF_6)_2(H_2O)_2\}_n$ (**2**) and $\{[Zn_3(4,4'\text{-bpy})_4(\mu\text{-}O_2CCH_2CH_3)_4](ClO_4)_2(4,4'\text{-bpy})_2(H_2O)_4\}_n$ (**3**) have been synthesized and characterized and their thermal stability has been examined.

Results and discussion

Crystal structure of $\{[Zn_3(4,4'\text{-bpy})_{3.5}(\mu\text{-}O_2CH)_4(H_2O)_2](ClO_4)_2(H_2O)_2\}_n$ (1)

The 3D molecular structure of compound **1** exhibits four different types of zinc(II) ions, each with octahedral N_2O_4 coordination environments (Fig. 1). The basal plane of the octahedron around Zn1 is formed by four oxygen atoms belonging to three formato ligands. The axial positions are occupied by two pyridine N-donors from two different (bridging) **4,4′-bpy** moieties (for the atom Zn3, the **4,4′-bpy** units act as monodentate ligands; see green **4,4′-bpy** ligands in Fig. 2). The formato ligand [O2, O12] acts as a bridging μ-O,O′ ligand, connecting Zn1 to Zn3 (Fig. 1). The formato ligand [O3, O8] functions as a μ_3-O,O,O′ ligand, bridging Zn1 and Zn3 and connecting the {Zn1, O3, Zn3} unit to an adjacent Zn4 ion

[a]*Department of Chemistry, Faculty of Science, Khon Kaen University, Khon Kaen, 40002, Thailand. E-mail: sujittra@kku.ac.th*
[b]*Department of Chemistry, Faculty of Science, Mahidol University, Bangkok, 10400, Thailand*
[c]*Department of Chemistry, Faculty of Science, Prince of Songkla University, Hatyai Songkla, 90112, Thailand*
[d]*Department of Physics, Faculty of Science and Technology, Thammasat University Rangsit, Pathumthani, 12121, Thailand*
[e]*ALS Berkeley Lab, 1 Cyclotron Road, MS-400, Berkeley, CA, 94720, USA*
[f]*Leiden Institute of Chemistry, Gorlaeus Laboratories, Leiden University, PO Box 9502, 2300, RA Leiden, The Netherlands*

† Electronic supplementary information (ESI) available: X-Ray powder diffraction patterns for compounds **1**–**3** (Fig. S1–S3). CCDC reference numbers 699370–699372. For ESI and crystallographic data in CIF or other electronic format see DOI: 10.1039/b901607d

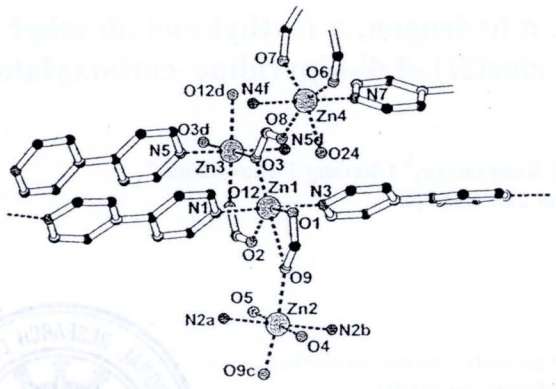

Fig. 1 Representation of the asymmetric unit of **1** showing the atom labeling scheme for the zinc(II) ions. The perchlorate anions, the lattice water molecules and the H atoms are not shown for clarity. Symmetry operations: a = 1 − *x*, *y*, 1/2 − *z*; b = 1 − *x*, *y*, 3/2 − *z*; c = 1 − *x*, −*y*, 1 − *z*; d = *x*, −*y*, −1/2 + *z*; f = 3/2 − *x*, 1/2 + *y*, 3/2 − *z*.

Table 1 Selected bond lengths (Å) and angles (°) for **1**[a]

Zn1–O1	2.100(3)	Zn2–O4	2.054(5)
Zn1–O2	2.048(3)	Zn2–O5	2.062(5)
Zn1–O3	2.082(3)	Zn2–O9	2.095(3)
Zn1–O9	2.639(3)	Zn2–O9c	2.095(3)
Zn1–N1	2.168(3)	Zn2–N2a	2.198(4)
Zn1–N3	2.171(3)	Zn2–N2b	2.198(4)
Zn3–O3	2.149(3)	Zn4–O6	2.036(5)
Zn3–O3d	2.149(3)	Zn4–O7	2.065(4)
Zn3–O12	2.082(3)	Zn4–O8	2.192(3)
Zn3–O12d	2.082(3)	Zn4–O24	2.144(4)
Zn3–N5	2.126(3)	Zn4–N4f	2.150(4)
Zn3–N5d	2.126(3)	Zn4–N7	2.163(4)
O1–Zn1–O3	122.98(11)	O4–Zn2–O9	97.25(9)
O3–Zn1–O2	100.69(12)	O9–Zn2–O5	82.75(9)
O2–Zn1–O9	83.07(9)	O5–Zn2–O9c	82.75(9)
O9–Zn1–O1	53.31(9)	O9c–Zn2–O4	97.25(9)
N1–Zn1–N3	175.19(15)	N2a–Zn2–N2b	180
O3–Zn3–O12	87.99(11)	O6–Zn4–O7	114.80(18)
O12–Zn3–O3d	92.01(11)	O7–Zn4–O8	84.76(13)
O3d–Zn3–O12d	87.99(11)	O8–Zn4–O24	77.31(13)
O12d–Zn3–O3	92.01(11)	O24–Zn4–O6	83.12(18)
N5–Zn3–N5d	180	N4f–Zn4–N7	178.21(16)

[a] Symmetry operations: a = 1 − *x*, *y*, 1/2 − *z*; b = 1 − *x*, *y*, 3/2 − *z*; c = 1 − *x*, −*y*, 1 − *z*; d = *x*, −*y*, −1/2 + *z*; f = 3/2 − *x*, 1/2 + *y*, 3/2 − *z*.

(through the oxygen atom O8). The third formato ligand [O1, O9] is chelating the atom Zn1 (Fig. 1) and is coordinated as well (through the atom O9) to a neighbouring Zn2 ion, thus acting as a μ-O,O′,O′ ligand.

The Zn–O and Zn–N bond distances are in normal ranges for this type of chromophore (Table 1).[21,24] The coordination angles, varying from 53.31(9) to 122.98(11)° (Table 1), reflect a strong distortion of the octahedron which is principally due to the very small bite angle of the chelating formato ligand.

The basal plane of the octahedron around Zn2 is constituted of two oxygen atoms (O9 and O9c) from two μ-O,O′,O′-formato ligands and two water oxygen atoms (O4 and O5). Zn2 lies on a two-fold axis and is coordinated by two different **4,4′-bpy** moieties (N2a and N2b) at the axial positions. The Zn–O and Zn–N bond distances can be considered as normal for this type of coordination environment (Table 1).[25] The basal angles ranging from 82.75(9) to 97.25(9)° indicate a distortion of the octahedral geometry, attributed to constraints induced by the bridging of the μ-O,O′,O′-formato ligands to Zn1.

The N_2O_4 coordination environment around the Zn3 ion, which lies on an inversion centre, is an almost perfect octahedron (the basal angles vary from 87.99(11) to 92.01(11); Table 1), with four in-plane oxygen atoms belonging to distinct formato ligands (O3, O12, O3d and O12d; Fig. 1). The axial positions are occupied by the nitrogen atoms N5 and N5d from two **4,4′-bpy** ligands. The Zn–O and Zn–N bond lengths are in common ranges.[21]

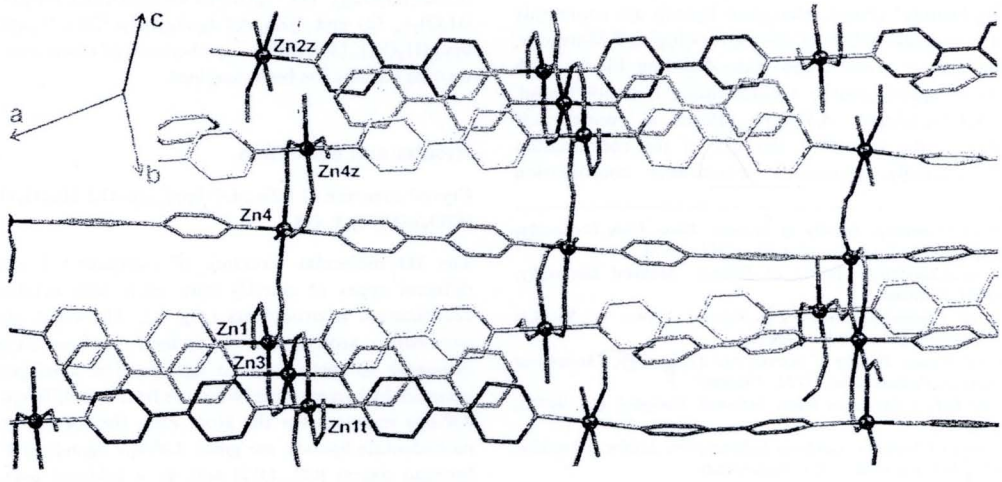

Fig. 2 3D coordination network of Zn^{II}, 4,4′-bipyridine and formate. The **4,4′-bpy** ligands involved in the formation of trinuclear zinc units are shown in blue, green and orange for comparison with compounds **2** and **3**. The **4,4′-bpy** ligands generating a 1D chain are depicted in red. Symmetry operations: t = 1/2 − *x*, −1/2 + *y*, 1/2 − *z*; *z* = 1 − *x*, y, 3/2 − *z*.

The distorted octahedral geometry around Zn4 (the basal angles range from 77.31(13) to 114.80(18)°) is most likely due to the bite angle of the μ-O,O′-formato ligands (oxygen atoms O6 and O7), connecting Zn4 to a symmetry-related Zn4 ion (see Fig. 2). The Zn–O and Zn–N bond distances are in normal ranges.[25]

The self-assembly between these bridging N- and O-ligands and zinc(II) ions gives rise to a remarkable 3D architecture (Fig. 2). The metal–organic framework is formed from trinuclear [Zn1, Zn3, Zn1] clusters which are connected through two **4,4′-bpy** ligands (yellow and blue **4,4′-bpy** ligands in Fig. 2) to the Zn2 and Zn4 ions, generating 1D, triple-stranded infinite chains. These chains showing π–π interactions between three **4,4′-bpy** units (with centroid-to-centroid distances ranging from 3.491(4) to 3.839(4) Å) are connected to each other *via* a different infinite single chain exhibiting the sequence {Zn1, Zn4, Zn4, Zn1, Zn2,...} (chain built from the orange **4,4′-bpy** ligands in Fig. 2). This spatial arrangement produces a unique heptanuclear coordination metallacycle (Fig. 3).

The organization of these heptanuclear motifs in the crystal lattice gives rise to the formation of channels which are filled by disordered perchlorates and water molecules (Fig. 4).

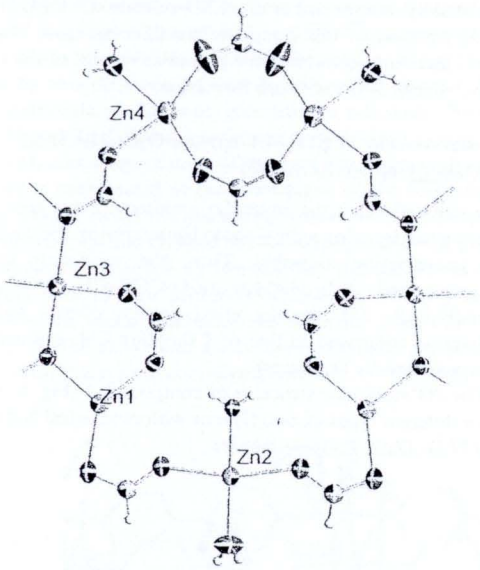

Fig. 3 Heptanuclear building unit constituting the channel walls in **1**.

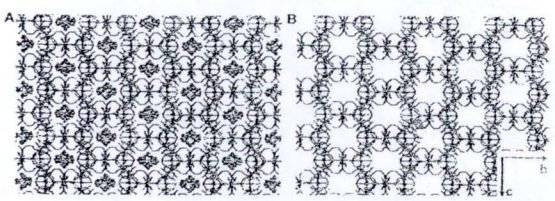

Fig. 4 (A) Channels filled with disordered perchlorate anions (shown in the space-filling mode) and water molecules. (B) Empty channels for compound **1**.

Crystal structure of {[Zn_3(4,4′-bpy)$_3$(μ-O_2CCH_3)$_4$(H_2O)$_2$](PF_6)$_2$(H_2O)$_2$}$_n$ (2)

The simple replacement of formate by acetate during the synthetic procedure (used to prepare **1**) produces significant structural changes in the crystal lattice of the resulting coordination compound {[Zn_3(**4,4′-bpy**)$_3$(μ-O_2CCH_3)$_4$(H_2O)$_2$](PF_6)$_2$(H_2O)$_2$}$_n$ (**2**). As is shown in Fig. 5, **2** only exhibits two types of zinc(II) ions, namely Zn1 and Zn2 (instead of four different zinc ions for compound **1**; see above).

Zn1 is characterized by a strongly distorted octahedral coordination environment, owing to the small bite angle of the μ-O,O′,O′ bridging mode of one of the two acetato ligands (the angle O3–Zn1–O4 is only 58.34(12)°; Table 2). The basal plane is constituted of four oxygen atoms belonging to two acetato ligands (O1, O3 and O4) and one water molecule (O5). The octahedron is completed by two **4,4′-bpy** nitrogen atoms (N1 and N2a), at the axial positions. The Zn–O and Zn–N bond distances can be considered as normal for this type of ZnN_2O_4 coordination environment (Table 2).

Zn2 lies on an inversion centre. The coordination environment around the Zn2 ion is an almost perfect octahedron, since the basal angles, varying from 87.73(13) to 92.27(13)°, are close to the ideal value of 90°. At the basal plane, Zn2 is coordinated by four oxygen atoms (O2, O3, O2c and O3c) from different acetato ligands. The axial positions are occupied by nitrogen atoms N3

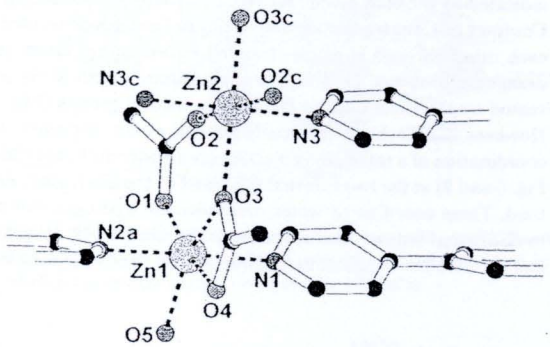

Fig. 5 Representation of the asymmetric unit of **2** showing the atom labeling scheme for the zinc(II) ions. The hexafluoridophosphate anions, the lattice water molecules and the H atoms are not shown for clarity. Symmetry operations: a = x, $-y+1$, z; c = $1-x$, $1-y$, $1-z$.

Table 2 Selected bond lengths (Å) and angles (°) for **2**[a]

Zn1–O1	1.995(4)	Zn2–O2	2.076(3)
Zn1–O3	2.218(3)	Zn2–O3	2.160(3)
Zn1–O4	2.241(4)	Zn2–N3	2.177(4)
Zn1–O5	2.060(3)		
Zn1–N1	2.168(4)		
Zn1–N2a	2.211(4)		
O1–Zn1–O3	104.77(13)	O2–Zn2–O3	87.73(13)
O3–Zn1–O4	58.34(12)	O3–Zn2–O2c	92.27(13)
O4–Zn1–O5	92.86(13)	N3–Zn2–N3c	180
O5–Zn1–O1	104.03(13)		
N1–Zn1–N2a	178.29(12)		

[a] Symmetry operations: a = x, $-y+1$, z; c = $1-x$, $1-y$, $1-z$.

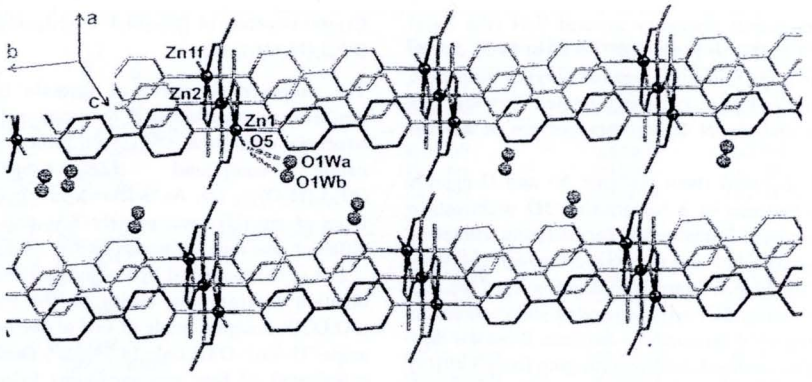

Fig. 6 1D coordination network in **2** of Zn^{II}, 4,4′-bipyridine and acetate. The **4,4′-bpy** ligands involved in the formation of trinuclear zinc units are shown in blue, green and orange for comparison with compounds **1** and **3**. Symmetry operations: a = $x, -y + 1, z$; b = $x, 1 + y, z$; f = $2 - x, 1 - y, 2 - z$.

and N3c, belonging to two **4,4′-bpy** ligands (lying on an inversion centre) at common distances.

Zn2 is bridged to two symmetry-related Zn1 ions *via* two μ-O,O′- and two μ-O,O′,O′-acetato ligands, generating a linear trinuclear [Zn1, Zn2, Zn1] cluster, analogous to the [Zn1, Zn3, Zn1] triad observed in **1** (see Fig. 2 and 6).

The [Zn1, Zn2, Zn1] clusters are connected to each other through coordination of the zinc ions by **4,4′-bpy** ligands, producing a 1D chain, constituted of three single zinc chains, indicated by the blue, green and yellow **4,4′-bpy** ligands in Fig. 6. Contrary to **1**, the triple-stranded chains in **2** are not connected to each other through a single-stranded coordination chain (see orange chain in Fig. 2). This interconnection is most likely prevented by the steric bulk of the acetato methyl groups (Fig. 7). However, the 1D chains are closely packed, which only allows the coordination of a small molecule, namely a water molecule (O5 in Fig. 6 and 7) at the two external positions of the [Zn1, Zn2, Zn1] triad. These coordinated water molecules are hydrogen-bonded to disordered lattice water molecules (O5···O1Wb = 2.717(16) Å and O5···O1Wa = 2.806(19) Å). Similarly to the ClO_4^- ions in **1**, the PF_6^- anions occupy the voids in the crystal lattice of **2** and apparently do not play a significant role in the formation of the framework (since their only interactions occur with the disordered lattice water molecules; the F···O contact distances are in the range 2.89(3)–2.98(2) Å). Actually, the compound $\{[Zn_3(\mathbf{4,4'\text{-}bpy})_3(\mu\text{-}O_2CCH_3)_4(H_2O)_2](ClO_4)_2(H_2O)\}_n$ has been previously reported by Woodward *et al.* (CSD refcode: CERFUB).[21] The X-ray structure of this compound exhibits the same 1D framework, therefore confirming the non-involvement of the PF_6^- or ClO_4^- anions in the network formation.

Crystal structure of $\{[Zn_3(4,4'\text{-bpy})_4(\mu\text{-}O_2CCH_2CH_3)_4](ClO_4)_2(4,4'\text{-bpy})_2(H_2O)_4\}_n$ (3)

The steric effect on the molecular architecture has been further investigated by using a propionato ligand during the synthesis of the coordination assembly. Thus, the solid-state structure of compound $\{[Zn_3(\mathbf{4,4'\text{-}bpy})_4(\mu\text{-}O_2CCH_2CH_3)_4](ClO_4)_2(\mathbf{4,4'\text{-}bpy})_2(H_2O)_4\}_n$ (**3**), bearing ethyl groups, shows significant differences compared to that of **2** (holding CH_3 groups) and **1** (characterized by H groups).

The 2D molecular structure of compound **3** (Fig. 8) exhibits three different types of zinc(II) ions with octahedral N_2O_4 (Zn1) and N_3O_3 (Zn2, Zn3) geometries.

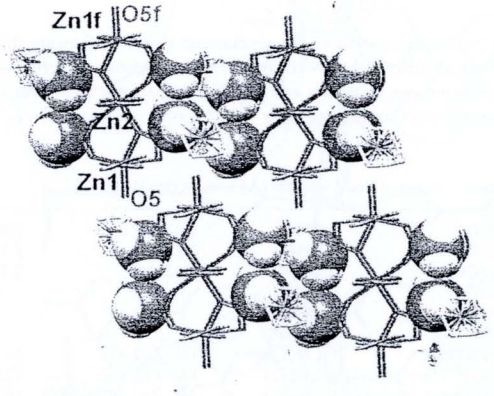

Fig. 7 Illustration of the steric bulk in **2** resulting from the acetato methyl groups (shown in the space-filling mode), which prevents the interconnection of the triple-stranded chains. Symmetry operation: f = $2 - x, 1 - y, 2 - z$.

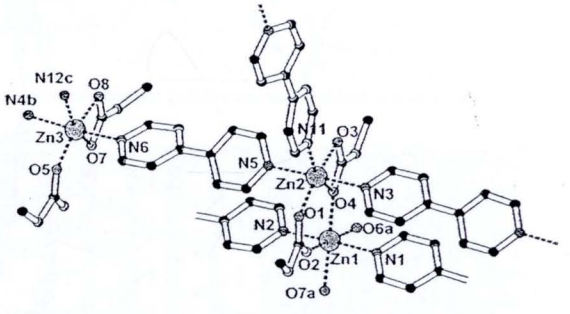

Fig. 8 Representation of the asymmetric unit of **3** showing the atom labeling scheme for the zinc(II) ions. The perchlorate anions, the lattice water molecules and the H atoms are not shown for clarity. Symmetry operations: a = $-x, -y + 1, -z$; b = $x-1, y, z - 1$; c = $-x, -y + 2, -z$.

Table 3 Selected bond lengths (Å) and angles (°) for 3[a]

Zn1–O2	2.119(2)	Zn2–O1	2.003(2)
Zn1–O4	2.133(2)	Zn2–O3	2.166(2)
Zn1–O6a	2.083(2)	Zn2–O4	2.218(2)
Zn1–O7a	2.152(2)	Zn2–N3	2.202(3)
Zn1–N1	2.174(3)	Zn2–N5	2.198(3)
Zn1–N2	2.167(3)	Zn2–N11	2.121(3)
Zn3–O5	1.995(2)	O2–Zn1–O4	89.74(9)
Zn3–O7	2.215(2)	O4–Zn1–O6a	89.58(10)
Zn3–O8	2.168(2)	O6a–Zn1–O7a	91.47(9)
Zn3–N6	2.206(3)	O7a–Zn1–O2	89.22(9)
Zn3–N4b	2.198(3)	N1–Zn1–N2	176.37(11)
Zn3–N12c	2.108(3)		
O1–Zn2–O4	105.33(9)	O5–Zn3–O7	103.28(9)
O4–Zn2–O3	59.55(9)	O7–Zn3–O8	59.57(9)
O3–Zn2–N11	95.36(10)	O8–Zn3–N12c	96.89(10)
N11–Zn2–O1	99.75(11)	N12c–Zn3–O5	100.31(11)
N3–Zn2–N5	178.24(11)	N6–Zn3–N4b	175.86(11)

[a] Symmetry operations: a = $-x$, $-y+1$, $-z$; b = $x-1$, y, $z-1$; c = $-x$, $-y+2$, $-z$; d = $-x+1$, $-y+1$, $-z+1$.

Zn1 exhibits an almost perfect octahedral environment with basal angles ranging from 89.22(9) to 91.47(9)° (Table 3). The basal plane is constituted of four oxygen atoms belonging to two μ-O,O′-propionato ligands (O2 and O6a) and two μ-O,O′,O′-propionato ligands (O4 and O7a). The axial positions are occupied by two different **4,4′-bpy** ligands which connect Zn1 to symmetry-related Zn1 ions, generating a polymeric chain. The Zn–N and Zn–O bond lengths are comparable to those of the ZnN_2O_4 coordination units of the previous compounds.

Zn2 is coordinated at the basal plane of the octahedron by three oxygen atoms and one nitrogen atom from two propionato ligands (O3, O4 and O1) and one **4,4′-bpy** ligand (N11). The axial positions are occupied by two **4,4′-bpy** ligands (N3 and N5), linking Zn2 to two symmetry-related Zn3 ions, generating a polymeric chain exhibiting the sequence {Zn2, Zn3, Zn2, Zn3,...}. The Zn–O and Zn–N bond distances are in normal ranges for this type of coordination moiety.[24,26] The basal angles varying from 59.55(9) to 105.33(9)° (Table 3) are indicative of a strong distortion of the octahedron, attributed to the small bite angle of the μ-O,O′-propionato ligand (O4–Zn2–O3 = 59.55(9)°).

The coordination environment around the Zn3 ion is comparable to that of Zn2. The ZnN_3O_3 unit exhibits analogous Zn–O

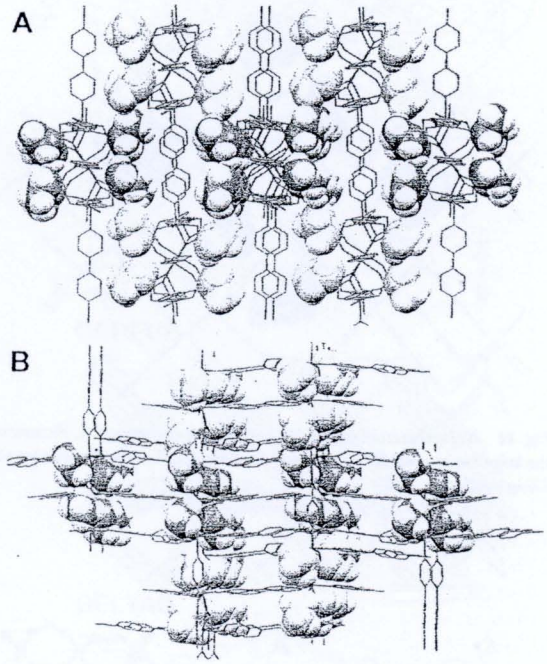

Fig. 10 Illustrations of the steric hindrance due to the propionato ethyl groups (shown in the space-filling mode, in grey and light blue) in **3**, which prevents close contacts between the 1D chains.

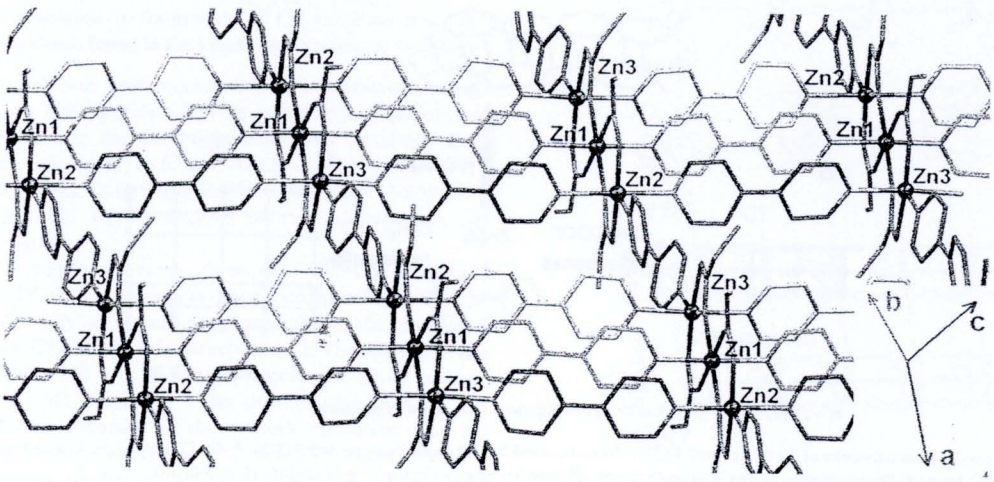

Fig. 9 2D coordination network in **3** of Zn^{II}, 4,4′-bipyridine and propionate. The **4,4′-bpy** ligands involved in the formation of trinuclear zinc units are shown in blue, green and orange for comparison with compounds **1** and **2**. The **4,4′-bpy** ligands connecting 1D three-leg ladders are shown in red.

and Zn–N bond lengths (to those of Zn2), which can be considered as normal (Table 3).[27] Similarly to Zn2, the coordination geometry around Zn3 is a strongly distorted octahedron, resulting from the small O7–Zn3–O8 angle of 59.57(9)° characterizing the coordination of the propionato ligand (Fig. 8).

The trinuclear [Zn1, Zn2, Zn3] clusters are connected to each other, in a head-to-tail fashion, through the coordination of the zinc ions by **4,4′-bpy** ligands, producing a 1D chain exhibiting the sequence {Zn1, Zn1, Zn1,...} for the central metal ion and { Zn2, Zn3, Zn2, Zn3,...} for the external zinc ions. This arrangement gives rise to triple-stranded chains, illustrated by the blue, green and yellow **4,4′-bpy** ligands in Fig. 9. These coordination polymeric chains are closely related to those observed for compound **2** (see Fig. 6 and 9) and reassemble part of the network of compound **1** (see Fig. 2 and 9). In contrast to the methyl groups in **2**, the ethyl groups of the propionato ligands in **3** do not allow a close packing of the triple-stranded polymeric chains (see Fig. 7 and 10), as the result of steric constraints. Consequently, the trinuclear zinc(II) units in **3** are more separated from each other than those in **2** (Fig. 7 and 10A). Indeed, the shorter intermolecular Zn···Zn separation distance is 9.391(3) Å for compound **3**, while the shorter intermolecular Zn···Zn distance is 5.557(3) Å for **2**.

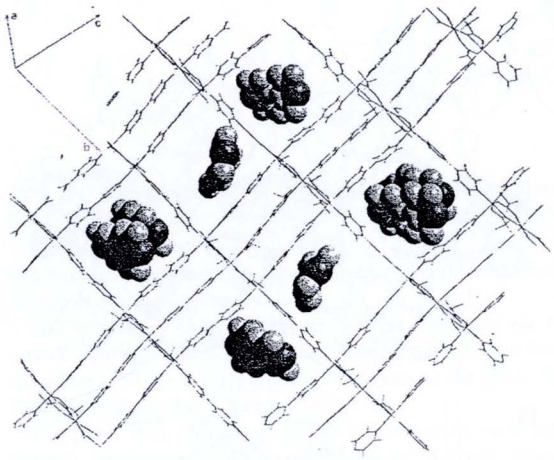

Fig. 11 Representation of the 2D network of compound **3**, illustrating the large cavities which contain non-coordinated **4,4′-bpy** ligands (space-filling mode).

This spatial organization allows the coordination of **4,4′-bpy** ligands at the two external positions of the trizinc moieties (orange **4,4′-bpy** ligands coordinated to Zn3 and Zn2; Fig. 9), connecting the triple-stranded chains to each other to form a 2D network. The herringbone-type architecture (Fig. 10A and 11) exhibit large cavities that can accommodate bulky guest molecules, namely non-coordinated **4,4′-bpy** ligands which are hydrogen-bonded to lattice water molecules (N10···O1w = 2.960(8), N9···O4w = 2.908(7) Å and N8···O3w = 2.827(10) Å). In addition, these large voids contain disordered perchlorate anions, which do not significantly interact with the metal–organic framework, but are hydrogen bonded to lattice water molecules (O15···O2w = 2.889(12) Å, O12···O3w = 2.831(15) Å and O12b···O3w = 2.882(15) Å).

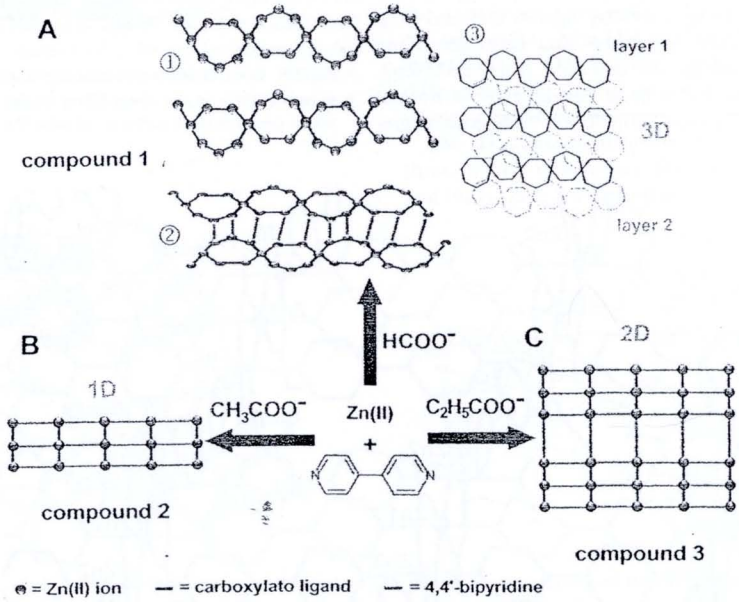

Fig. 12 Coordination networks of A) compound **1** (3D), B) compound **2** (1D) and C) compound 3 (2D). A-①: 1D chains packed in a parallel fashion, forming a 2D layer; A-②: connection of two chains through **4,4′-bpy** ligands; A-③: packing of slightly shifted layers.

Coordination networks

The use of slightly different carboxylato moieties as secondary co-ligands of [Zn(II)/**4,4′-bpy**] coordination units, applying the same reaction conditions, leads to the formation of drastically distinct networks (Fig. 12).

The combination [Zn^{II}/**4,4′-bpy**/formate] generates an intricate 3D framework (Fig. 12A). The bridging of zinc(II) ions by formato ligands produces a 1D chain constituted of heptanuclear rings (see Fig. 3 and 12A-①). These chains are arranged in a parallel fashion, resulting in a 2D layer. Each layer is linked to one layer above and to one layer below through coordinated 4,4′-bipyridines (red lines in Fig. 12A-②). Since each chain is connected to two chains above and to two chains below, this spatial organization creates a 3D framework of slightly shifted layers (Fig. 12A-③).

The sole replacement of formate by acetate results in the formation of 1D network (Fig. 12B). This simple framework is built from trinuclear acetato-bridged units that are linked to two adjacent ones, to form a three-leg ladder.

The use of propionate as co-ligand yields a 2D network (Fig. 12C) which presents similarities with the previous one. Actually, the framework of **3** contains the three-leg ladders observed in solid-state structure of **2**. These three-leg ladders are connected to each other *via* **4,4′-bpy** ligands (vertical red lines in Fig. 12C).

It should be noted that, albeit the three coordination networks are different, they show some common features. Indeed, all three structures exhibit trinuclear carboxylato-bridged moieties as secondary building units (SBUs). Moreover, infinite {–Zn–(4,4′-bpy)–}$_n$ chains are observed for the three compounds (see for instance, the red {–Zn4–(4,4′-bpy)–}$_n$ chains in Fig. 2, and the blue {–Zn1/Zn2–(4,4′-bpy)–}$_n$ chains in Fig. 6 and 9, respectively). Finally, one should notice that the zinc(II) ions have similar coordination environments, regardless of the carboxylato co-ligand used. Therefore, the structural diversity of the frameworks obviously originates from different steric constraints induced by the carboxylato ligands.

Comparison between the frameworks of 1, 2 and 3 and those of related compounds found in the Cambridge Structural Database

Eight coordination frameworks exclusively constructed from zinc(II) ions, 4,4′-bipyridine ligands and bridging carboxylato units are found in the Cambridge Structural Database (CSD ConQuest version 1.11; Refcodes: ALUPUS,[14,15,28] CERFOV,[21] CERFUB,[21] DELTAQ,[19] EYELID,[17] JODFIS,[13] NEWTIT[18] and QEQBIY[12]). Representations of these frameworks are shown in Fig. 13.

From the eight compounds, three, *i.e.* CERFOV, CERFUB and QEQBIY, show frameworks that are comparable to those of **2** and **3**. Actually, as already mentioned above, the compound with refcode CERFUB[21] is isostructural to **2**. The sole difference between CERFUB and **2** lies in the distinct lattice anions, respectively, ClO_4^- and PF_6^-. This demonstrates that the two anions have no influence on the network formation. The 2D triple-chain sheet architectures of CERFOV[21] and QEQBIY[12] are comparable to that of **3**. The remaining five compounds exhibit 1D networks (ALUPUS, EYELID, JODFIS and

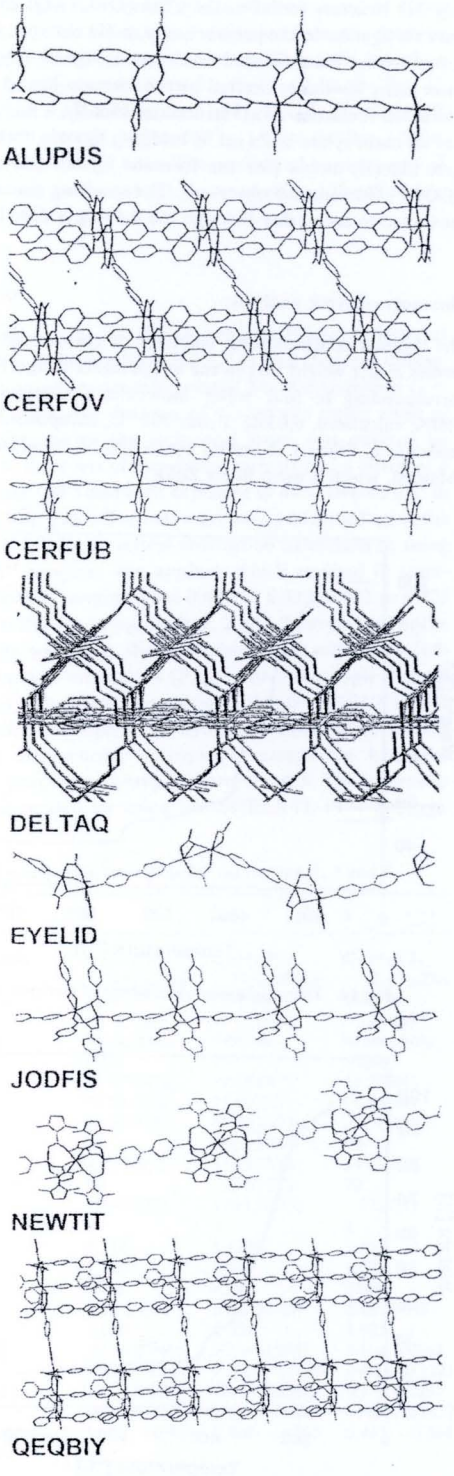

Fig. 13 Representations of the coordination networks exhibited by the seven [Zn^{II}/**4,4′-bpy**/carboxylato]-based compounds found in the CSD.

NEWTIT) or a 3D framework (DELTAQ). Interestingly, the only 3D structure found in the CSD (DELTAQ) contains formato co-ligands. In the present study, a 3D network is observed as well when formate is used as secondary ligand. Therefore, the lower steric hindrance exerted by the formato ligand appears to favour the formation of 3D structures. Finally, it has to be noted that all carboxylato units act as bridging ligands, linking two or three zinc(II) atoms (for the formato ligand, polymeric $Zn^{II}/HCOO^-$ structures are observed). The resulting zinc clusters are connected to each other through the 4,4′-bipyridine ligands.

Thermogravimetric analysis

The thermal decomposition behavior of compound **1** (Fig. 14) reveals a first weight loss in the temperature range 143–201 °C, corresponding to four water molecules (experimental value, 5.50%; calculated, 6.03%). From 202 °C, compound **1** starts to decompose. When **1** is heated up to 800 °C, a white residue is obtained, which is most likely ZnO.

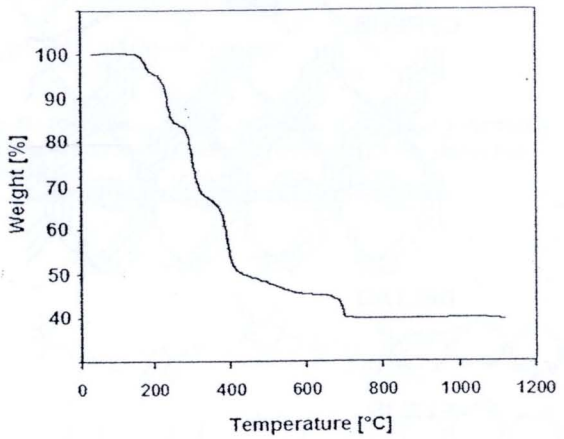

Fig. 14 Thermogravimetric analysis of compound **1**.

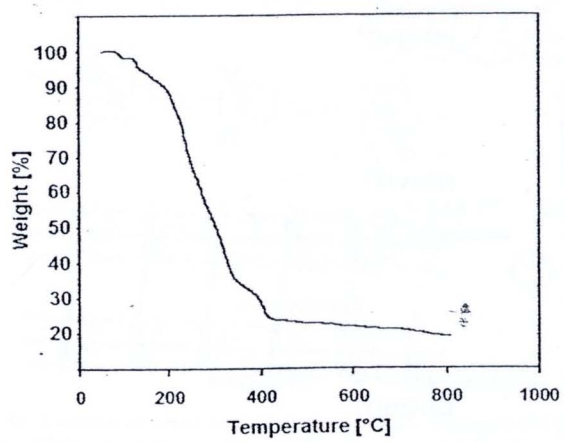

Fig. 15 Thermogravimetric analysis of compound **2**.

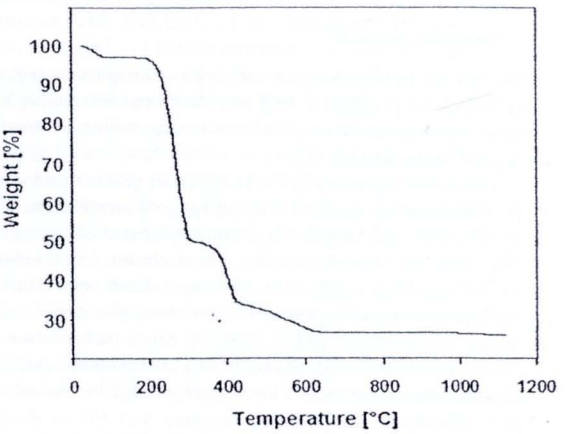

Fig. 16 Thermogravimetric analysis of compound **3**.

The thermogravimetric analysis of compound **2** (Fig. 15) shows a first weight loss in the temperature range 71–170 °C, characterizing the loss of four water molecules (experimental value, 5.82%; calculated, 5.70%). In the temperature range 171–429 °C, the decomposition of the coordination material is observed. As for **1**, a white residue (ZnO) is obtained when **2** is heated to 800 °C.

The thermal analysis of **3** (Fig. 16) exhibits a two-stage decomposition of the material. A first weight loss of 3.50% is observed in the temperature range 92–195 °C, which corresponds to the release of four lattice water molecules (calculated 4.15%). In the temperature range 196–630 °C, compound **3** degrades. As for compounds **1** and **2**, a white residue (ZnO) is obtained when the sample is heated to 800 °C.

Conclusions

One of the most important challenges that remains in crystal engineering is crystal structure prediction. As properly stated by Desiraju,[29] the main objective of the crystal engineering chemist is to try to understand intermolecular interactions in the context of crystal packing and to use such knowledge to rationally design new materials with anticipated molecular structures and desired physical and chemical properties.

In the present study, the influence of small secondary ligands, namely common monocarboxylato ligands, on the overall solid-state structure of [zinc(II)–4,4-bpy–carboxylato] coordination compounds has been investigated. This study shows that the change from a formato ligand to an acetato and a propionato ligand gives rise to the formation of drastically distinct metal–organic frameworks, as the result of the different steric bulk of the carboxylato unit involved. Such studies are of great interest for the crystal engineering chemist, as they contribute to increase the knowledge about crystallization processes and molecular structure prediction.

Experimental

All starting materials were commercially available and used as received. IR spectra were recorded on a Perkin-Elmer Spectrume

One FTIR spectrophotometer as KBr discs in the range 4000–450 cm^{-1}. C, H, and N analyses were performed on a Perkin-Elmer PE2400 CHNS/O. Thermogravimetric analyses were carried out using a Perkin-Elmer Pyris Diamond analyzer in flowing nitrogen at a heating rate of 10 °C min^{-1}. X-ray powder diffraction (XRPD) data for **1**–**3** were obtained using a Phillips Xpert Pro equipped with an X'celerator, with Cu Kα radiation ($\lambda \approx 1.5408$ Å), in the 2θ range 10–45. The diffraction patterns were recorded at room temperature (see Fig. S1–S3, ESI).†

Synthesis of $\{[Zn_3(4,4'\text{-bpy})_{3.5}(\mu\text{-}O_2CH)_4(H_2O)_2](ClO_4)_2(H_2O)_2\}_n$ (1)

An aqueous solution (10 mL) of $Zn(NO_3)_2 \cdot 6H_2O$ (0.302 g, 1.0 mmol) was added to an ethanolic solution (10 mL) of **4,4'-bpy** (0.157 g, 1.0 mmol). An aqueous solution (10 mL) of NaO_2CH (sodium formate; 0.149 g, 2.0 mmol) was subsequently added, followed by 0.141 g of $KClO_4$ (1.0 mmol) under continuous stirring. The resulting colourless solution was allowed to stand unperturbed for the slow evaporation of the solvent at room temperature. After several days, colourless crystals were obtained. The crystals were filtered, washed with the mother liquid and dried in air. Yield = 0.262 g (66% based on Zn). Elemental analyses calculated for $C_{39}H_{40}Cl_2N_7O_{20}Zn_3$: C, 39.24; H, 3.38; N, 8.21. Found: C, 39.22; H, 3.31; N, 8.22%. IR data (cm^{-1}): 3400s, 1609s, 1588s, 1536w, 1413m, 1384m, 1348w, 1224w, 1117s, 1089s, 807s, 630s. The purity and homogeneity of compound **1** were confirmed by X-ray powder diffraction (see Fig. S1).†

Synthesis of $\{[Zn_3(4,4'\text{-bpy})_3(\mu\text{-}O_2CCH_3)_4(H_2O)_2](PF_6)_2(H_2O)_2\}_n$ (2)

An aqueous solution (15 mL) of $Zn(NO_3)_2 \cdot 6H_2O$ (0.306 g, 1.0 mmol) was added to a solution of **4,4'-bpy** (0.157 g, 1.0 mmol) in ethanol (10 mL). Next, an aqueous solution (20 mL) of NaO_2CCH_3 (sodium acetate; 0.138 g, 2.0 mmol) and an aqueous solution (10 mL) of KPF_6 (0.185 g, 1.0 mmol) were added under continuous stirring. A few drops of CH_3COOH 98% were subsequently added to the reaction mixture, yielding a clear colorless solution. This solution was allowed to stand unpertubed for the slow evaporation of the solvent at room temperature, producing colorless needle crystals of **2** after a few days. Yield = 0.290 g (70% based on Zn). Elemental analyses calculated for $C_{38}H_{44}F_{12}N_6O_{12}P_2Zn_3$: C, 36.14; H, 3.51; N, 6.66. Found: C, 36.41; H, 3.24; N, 6.30%. IR data (cm^{-1}): 3400s, 3045s, 1603s, 1520s, 1490s, 1419s, 133m, 1219s, 1070s, 1195s, 1100s, 1074s 1046m, 1015m, 846s, 838s, 643m, 630m, 560s. The purity and homogeneity of compound **2** were confirmed by X-ray powder diffraction (see Fig. S2).†

Synthesis of $\{[Zn_3(4,4'\text{-bpy})_4(\mu\text{-}O_2CCH_2CH_3)_4](ClO_4)_2(4,4'\text{-bpy})_2(H_2O)_4\}_n$ (3)

An aqueous solution (10 mL) of $Zn(NO_3)_2 \cdot 6H_2O$ (0.313 g, 1.0 mmol) was added to a solution of **4,4'-bpy** (0.158 g, 1.0 mmol) in ethanol (10 mL). Subsequently, an aqueous solution (10 mL) of $NaCOOCH_2CH_3$ (sodium propanoate; 0.201 g, 2.0 mmol) was added, followed by $KClO_4$ (0.152 g, 1.0 mmol) under continuous stirring. Next, a few drops of CH_3CH_2COOH 98% were added, yielding a clear colourless solution, which was allowed to stand unperturbed for the slow evaporation of the solvent at room temperature. Colorless crystals were collected from the solution by filtration after several days. Yield = 0.385 g (68% based on Zn). Elemental analyses calculated for $C_{72}H_{76}Cl_2N_{12}O_{20}Zn_3$: C, 50.97; H, 4.52; N, 9.91. Found: C, 51.19; H, 4.84; N, 9.91%. IR data (cm^{-1}): 3392s, 1609s, 1578s, 1552s, 1466m, 1419m, 1222w, 1107s, 1067s, 1046m, 808s, 631s. The purity and homogeneity of compound **3** were confirmed by X-ray powder diffraction (see Fig. S3).†

Crystallography

The X-ray single-crystal data for all compounds were collected at 293(2) K on a 1 K Bruker SMART CCD area detector diffractometer using graphite monochromated Mo Kα radiation ($\lambda = 0.71073$ Å) at a detector distance of 4.5 cm and swing angle of −35°. A hemisphere of the reciprocal space was covered by combination of three sets of exposures; each set had a different ϕ angle (0, 88, and 180°) and each exposure of 40 s covered 0.3° in ω. Data reduction and cell refinements were performed using the program SAINT.[30] An empirical absorption correction by using the SADABS[31] program was applied, which resulted in transmission coefficients ranging from 0.690 to 0.820, 0.642 to 0.823 and 0.600 to 0.680 for compounds **1**, **2** and **3**, respectively. The structures were solved by direct methods and refined by full-matrix least-squares method on $(F_{obs})^2$ with anisotropic thermal parameters for all non-hydrogen atoms using the SHELXTL-PC V 6.12 software package.[32] All hydrogen atoms were located geometrically and refined isotropically except the hydrogen atoms of the propionate group in compound **3**. The molecular graphics were created by using the SHELXTL-PC[32] package.

Table 4 Crystal and refinement data for compounds **1**, **2** and **3**

Compound	1	2	3
Empirical formula	$C_{39}H_{40}Cl_2N_7O_{20}Zn_3$	$C_{38}H_{44}F_{12}N_6O_{12}P_2Zn_3$	$C_{72}H_{76}Cl_2N_{12}O_{20}Zn_3$
Formula weight	1193.79	1262.84	1696.46
T/K	293(2)	293(2)	293(2)
Crystal system	Monoclinic	Triclinic	Monoclinic
Space group	$C2/c$	$P\text{-}1$	$P2_1/c$
a/Å	26.8795(12)	10.6952(7)	18.506(4)
b/Å	19.1415(8)	11.4831(7)	18.838(4)
c/Å	21.2041(9)	11.7638(7)	25.568(5)
α/°	90	101.558(2)	90
β/°	122.078(2)	116.757(2)	119.90(3)
γ/°	90	95.574(2)	90
V/Å^3	9244.2(7)	1234.58(13)	7727(3)
Z	8	1	4
D_{calc}/g cm^{-3}	1.716	1.699	1.458
μ/mm^{-1}	1.748	1.619	1.071
$F(000)$	4856	638	3504
θ range/°	2.22–21.99	2.02–30.35	2.16–27.48
GOF	1.030	1.007	1.023
Final R indices[a]	$R1 = 0.0465$	$R1 = 0.0648$	$R1 = 0.0562$
$[I > 2\sigma(I)]$	$wR2 = 0.1116$	$wR2 = 0.1666$	$wR2 = 0.1223$
R indices (all data)	$R1 = 0.0623$	$R1 = 0.0895$	$R1 = 0.0897$
	$wR2 = 0.1206$	$wR2 = 0.1867$	$wR2 = 0.1332$
Largest difference peak and hole/e Å^{-3}	0.727, −0.981	1.460, −1.905	0.417, −0.564

[a] $R = \sum\|F_o\| - \|F_c\|/\sum\|F_o\|$, $R_w = [\sum w\{\|F_o\| - \|F_c\|\}^2/\sum w|F_o^2|^2]^{1/2}$.

The crystal and refinement details of all compounds are listed in Table 4.

For compound **1**, displacement parameter restrains were used in modelling the percholates and the bpy ligands. Even with these, the displacement parameter ratio (maximin) of a few atoms is around 4.5 : 1, and the anisotropic parameters for the perchlorate are larger than ideal. Geometric restrains were used in modelling the chlorates.

Acknowledgements

The authors are very grateful to the Higher Education Development Projects: The Royal Golden Jubilee Ph.D. Program (RGJ) and Khon Kean University for a research grant. Support of The Thailand Research Fund and the Center of Excellence for Innovation in Chemistry (PERCH-CIC), Commission on Higther Education, Ministry of Education is also gratefully acknowledged.

References

1 S. R. Batten, S. M. Neville and D. R. Turner, *Coordination Polymers: Design, Analysis and Application*, RSC Publishing, Cambridge, 2008.
2 B. Moulton and M. J. Zaworotko, *Chem. Rev.*, 2001, **101**, 1629–1658.
3 D. Bradshaw, J. E. Warren and M. J. Rosseinsky, *Science*, 2007, **315**, 977–980.
4 W. J. Shi, C. X. Ruan, Z. Li, M. Li and D. Li, *CrystEngComm*, 2008, **10**, 778–783.
5 L. Carlucci, G. Ciani and D. M. Proserpio, *Coord. Chem. Rev.*, 2003, **246**, 247–289.
6 L. Brammer, *Chem. Soc. Rev.*, 2004, **33**, 476–489.
7 M. L. Tong and X. M. Chen, *CrystEngComm*, 2000, **2**, 1–5.
8 M. Eddaoudi, H. L. Li and O. M. Yaghi, *J. Am. Chem. Soc.*, 2000, **122**, 1391–1397.
9 R. Robson, *J. Chem. Soc., Dalton Trans.*, 2000, 3735–3744.
10 O. M. Yaghi, M. O'Keeffe, N. W. Ockwig, H. K. Chae, M. Eddaoudi and J. Kim, *Nature*, 2003, **423**, 705–714.
11 M. J. Rosseinsky, *Microporous Mesoporous Mater.*, 2004, **73**, 15–30.
12 Y. Z. Zheng, M. L. Tong and X. M. Chen, *J. Mol. Struct.*, 2006, **796**, 9–17.
13 D. Y. Ma and G. H. Deng, *Acta Crystallogr., Sect. C: Cryst. Struct. Commun.*, 2008, **64**, M271–M273.
14 M. G. Amiri and A. Morsali, *Z. Anorg. Allg. Chem.*, 2006, **632**, 2491–2494.
15 B. Conerney, P. Jensen, P. E. Kruger, B. Moubaraki and K. S. Murray, *CrystEngComm*, 2003, **5**, 454–458.
16 X. J. Zhang, J. Y. Wu, M. L. Zhang, Y. P. Tian, M. H. Jiang, A. Usman, S. Chantrapromma and H. K. Fun, *Transit. Met. Chem.*, 2003, **28**, 707–711.
17 T. W. Lee, J. P. K. Lau and W. T. Wong, *Polyhedron*, 2004, **23**, 999–1002.
18 C. F. Wang, Z. Y. Zhu, Z. X. Zhang, Z. X. Chen and X. G. Zhou, *CrystEngComm*, 2007, **9**, 35–38.
19 X. H. Miao, H. P. Xiao and L. G. Zhu, *Acta Crystallogr., Sect. E: Struct. Rep. Online*, 2006, **62**, M1756–M1757.
20 B. H. Ye, M. L. Tong and X. M. Chen, *Coord. Chem. Rev.*, 2005, **249**, 545–565.
21 J. D. Woodward, R. V. Backov, K. A. Abboud and D. R. Talham, *Polyhedron*, 2006, **25**, 2605–2615.
22 L. G. Zhu, S. Kitagawa, H. Miyasaka and H. C. Chang, *Inorg. Chim. Acta*, 2003, **355**, 121–126.
23 L. G. Zhu and S. Kitagawa, *Inorg. Chem. Commun.*, 2002, **5**, 358–360.
24 Y. M. Dai, E. Ma, E. Tang, J. Zhang, Z. J. Li, X. D. Huang and Y. G. Yao, *Cryst. Growth Des.*, 2005, **5**, 1313–1315.
25 T. Ohmura, W. Mori, M. Hasegawa, T. Takei, T. Ikeda and E. Hasegawa, *Bull. Chem. Soc. Jpn.*, 2003, **76**, 1387–1395.
26 J. Tao, X. Yin, Y. B. Jiang, L. F. Yang, R. B. Huang and L. S. Zheng, *Eur. J. Inorg. Chem.*, 2003, 2678–2682.
27 D. J. Darensbourg, J. R. Wildeson and J. C. Yarbrough, *Inorg. Chem.*, 2002, **41**, 973–980.
28 J. Kim, U. Lee and B. K. Koo, *Bull. Korean Chem. Soc.*, 2006, **27**, 918–920.
29 G. R. Desiraju, *Angew. Chem., Int. Ed.*, 2007, **46**, 8342–8356.
30 *SAINT, Version 4 Software Reference Manual*, (1996) Siemens Analytical X-Ray Systems, Inc., Madison, WI, USA.
31 G. M. Sheldrick, *SADABS, Program for Empirical Absorption correction of Area Dectector*, 1996, University of Göttingen, Göttingen, Germany.
32 *SHELXTL, Version 6.12 Reference Manual*, 1997, Siemens Analytical X-Ray Systems, Inc., Madison, WI, USA.

CREATED USING THE RSC ARTICLE TEMPLATE (VER. 3.0) - SEE WWW.RSC.ORG/ELECTRONICFILES FOR DETAILS

ARTICLE TYPE

www.rsc.org/xxxxxx | XXXXXXXX

Catalytic properties of a series of coordination networks: cyanosilylation of aldehydes catalyzed by Zn(II)-4,4'-bpy-carboxylato complexes

Pongthipun Phuengphai,[a, b] Sujittra Youngme,*[a] Patrick Gamez[b] and Jan Reedijk[b]

Received (in XXX, XXX) xxxxx 2009, Accepted xxxx 2009
First published as an Advance Article on the web XXX

Three porous crystalline coordination polymers, *i.e.* the three-dimensional framework $\{[Zn_3(4,4'\text{-bpy})_{3.5}(\mu\text{-}O_2CH)_4(H_2O)_2](ClO_4)_2(H_2O)_2\}_n$ (**1**), the one-dimensional three-leg ladder $\{[Zn_3(4,4'\text{-bpy})_3(\mu\text{-}O_2CCH_3)_4(H_2O)_2](PF_6)_2(H_2O)_2\}_n$ (**2**), and the two-dimensional layered network $\{[Zn_3(4,4'\text{-bpy})_4(\mu\text{-}O_2CCH_2CH_3)_4](ClO_4)_2(4,4'\text{-bpy})_2(H_2O)_4\}_n$ (**3**), have been investigated. All networks exhibit voids that contain the counter-ions and guest molecules, namely water for compounds **1** and **2**, and water/4,4'-bpy for compound **3**. In addition, compounds **2** and **3** are further stabilized by hydrogen bonds and π-π stacking interactions to form intricate supramolecular frameworks. The removal and reintroduction of guest water molecules for compounds **2** and **3** have been explored for their dynamic structural transformation. Interestingly, all Zn(II) compounds are active heterogeneous catalysts for the high-yield cyanosilylation of acetaldehyde in dichloromethane.

Introduction

Porous coordination polymers (PCPs), also known as metal-organic frameworks (MOFs), may be assembled from various molecular building blocks; therefore, diverse architectures and functions can be achieved.[1-3] MOFs may find potential applications in molecular adsorption and separation processes,[1-3] ion-exchange,[4-6] catalysis,[7] sensor technology,[8] and optoelectronics.[9] The design of porous coordination polymers does not only allow the preparation of light materials with high porosity, but also the generation of desirable regular networks. PCPs are engineered by linking building blocks at their coordination sites via multifunctional linkers into perfect and esthetic architectures, whose topology is pre-defined by the arrangement of the coordination sites and the orientation and number of the binding groups in the linker. Despite extensive studies, applications of porous compounds are still quite limited compared to that of zeolites. Inorganic materials with inner cavities, such as zeolites are known to bind many organic molecules in the hollow spaces and often exhibit unique catalytic properties for a number of organic reactions, in which high regioselectivity, stereoselectivity, and shape selectivity are observed.[10-15] Reports of catalytic studies involving coordination polymers have been relatively scarce.[16-29] While most of these investigations have dealt with some significant successes in enantioselective catalysis,[17, 18] there has been little focus thus far on probing the selectivity with substrates of comparable size to the pore dimensions.[27, 29]

Only few catalytic applications of carboxylato-bridged porous coordination polymers have been reported.[4-7] The catalytic and dynamic structural transformation of three coordination polymeric architectures for which preliminary results were published,[30] namely the 3D $\{[Zn_3(4,4'\text{-bpy})_{3.5}(\mu\text{-}O_2CH)_4(H_2O)_2](ClO_4)_2(H_2O)_2\}_n$ (**1**), the 1D $\{[Zn_3(4,4'\text{-bpy})_3(\mu\text{-}O_2CCH_3)_4(H_2O)_2](PF_6)_2(H_2O)_2\}_n$ (**2**) and the 2D $\{[Zn_3(4,4'\text{-bpy})_4(\mu\text{-}O_2CCH_2CH_3)_4](4,4'\text{-bpy})_2(ClO_4)_2(H_2O)_4\}_n$ (**3**), are herein reported.

[a] *Department of Chemistry, Faculty of Science, Khon Kaen University, Khon Kaen 40002, Thailand. E-mail: sujittra@kku.ac.th*
[b] *Leiden Institute of Chemistry, Gorlaeus Laboratories, Leiden University, PO Box 9502, 2300 RA Leiden, The Netherlands*

Experimental Section

Preparation of the coordination polymers

Synthesis of $\{Zn_3(4,4'\text{-bpy})_{3.5}(\mu\text{-}O_2CH)_4(H_2O)_2(ClO_4)_2(H_2O)_2\}_n$ (1)[30]

An aqueous solution (10 mL) of $Zn(NO_3)_2{\cdot}6H_2O$ (0.302 g, 1.0 mmol) was added to an ethanolic solution (10 mL) of 4,4'-bpy (0.157 g, 1.0 mmol). An aqueous solution (10 mL) of NaCOOH (sodium formate; 0.149 g, 2.0 mmol) was subsequently added, followed by 0.141 g of $KClO_4$ (1.0 mmol) under continuous stirring. The resulting colorless solution was allowed to stand unperturbed for the slow evaporation of the solvent at room temperature. After several days, colorless crystals were obtained. The crystals were filtered, washed with the mother liquid and dried in air. Yield = 68 %.

Synthesis of $\{Zn_3(4,4'\text{-bpy})_3(\mu\text{-}O_2CCH_3)_4(H_2O)_2(PF_6)_2(H_2O)_2\}_n$ (2) and $\{Zn_3(4,4'\text{-bpy})_4(\mu\text{-}O_2CCH_2CH_3)_4(4,4'\text{-bpy})_2(ClO_4)_2(H_2O)_4\}_n$ (3)[30]

Complexes **2** and **3** have also been obtained following the synthetic procedure applied for compound **1**, using sodium acetate for **2** and sodium propionate for **3** in place of sodium formate (compound **1**). Yield = 78 % (**2**) and 70 % (**3**).

Synthesis of $\{Zn_3(4,4'\text{-bpy})_{3.5}(\mu\text{-}O_2CH)_4(H_2O)_2(ClO_4)_2(H_2O)_2\}_n$ (1) doped with Cu^{2+} (1a) and Mn^{2+} (1b)

An aqueous solution (10 mL) of $Zn(NO_3)_2{\cdot}6H_2O$ (0.308 g, 1.0 mmol) was added to an ethanolic solution (10 mL) of 4,4'-bpy (0.158 g, 1.0 mmol). An aqueous solution (10 mL) of NaCOOH (sodium formate; 0.148 g, 2.0 mmol) was subsequently added, followed by 0.141 g of $KClO_4$ (1.0 mmol) and 0.003 g (0.002 mmol) of $Cu(NO_3)_2{\cdot}3H_2O$ (or 0.003 g $Mn(NO_3)_2{\cdot}4H_2O$ (0.002 mmol)) under continuous stirring. The resulting solution was allowed to stand unperturbed for the slow evaporation of the solvent at room temperature. After several days, light-green crystals of **1a** were obtained (light-pink crystals for **1b**). The crystals were filtered, washed with the mother liquor and dried in air. Yield = 66 %. The IR spectra of **1a** and **1b** are similar to that of **1**.

Synthesis of $\{Zn_3(4,4'\text{-bpy})_3(\mu\text{-}O_2CCH_3)_4(H_2O)_2(PF_6)_2(H_2O)_2\}_n$ (2) and $\{Zn_3(4,4'\text{-bpy})_4(\mu\text{-}O_2CCH_2CH_3)_4(4,4'\text{-bpy})_2(ClO_4)_2(H_2O)_4\}_n$ (3) doped with Cu^{2+} and Mn^{2+}, 2a, 2b, 3a and 3b

CREATED USING THE RSC ARTICLE TEMPLATE (VER. 3.0) - SEE WWW.RSC.ORG/ELECTRONICFILES FOR DETAILS

ARTICLE TYPE www.rsc.org/xxxxxx | XXXXXXXX

Complexes **2a**, **2b**, **3a** and **3b** can also be obtained applying the same synthetic procedure as for **1a** and **1b**, using sodium acetate and Cu^{2+} for **2a** (Mn^{2+} for **2b**) and potassium propionate and Cu^{2+} for **3a** (Mn^{2+} for **3b**). The IR spectra of the doped compounds are comparable to those of the corresponding parent compounds, respectively **2** and **3**.

Characterization

FTIR spectra were recorded on a Perkin–Elmer Paragon 1000 FTIR spectrophotometer, equipped with a Golden Gate ATR device, using the reflectance technique (4000–300 cm^{-1}). Elemental analyses for C, H and N were performed with a Perkin–Elmer 2400 analyzer. Thermogravimetric analyses were carried out using a Perkin-Elmer Pyris Diamond analyzer in flowing nitrogen at a heating rate of 10 °C min^{-1}. The X-band powder EPR spectra were obtained on polycrystalline samples at room temperature and at 77 K with a Bruker EMXplus spectrometer with DPPH (g = 2.0036) as a reference. X-ray powder diffraction (XRPD) data were recorded at room temperature using a Phillips Xpert Pro equipped with an X'celerator, with Cu Kα radiation ($\lambda \approx 1.5408$ Å), in the 2θ range 10-45°.

Catalytic Reactions

A typical cyanosilylation reaction was performed as follows: 40 mg (0.006 mmol, 0.2 mmol of Zn) of MOF catalyst was suspended in 5mL of dry dichloromethane (CH_2Cl_2) or tetrahydrofuran (THF), followed by the addition of the aldehyde (1.5 mmol) and trimethylsilyl cyanide (3 mmol). The reaction mixtures were stirred at room temperature under argon. The reaction conversions were determined by gas chromatography (GC) analysis. The catalytic recyclability was checked three times with the same batch of catalyst, and no obvious decrease in activity was observed. For the filtration test, the catalyst was separated after a reaction time of 5 h and the solution was divided into two equal portions. Hereafter, one portion was stirred with fresh catalyst, while the second one was stirred without MOF catalyst.

Results and Discussion

Synthesis and Structure

Crystalline materials were obtained for all three compounds prepared from zinc(II) ions, 4,4'-bpy and carboxylato ligands in ethanol/H_2O solvent mixture. Other solvent combinations were used, *i.e.* methanol/H_2O and acetone/H_2O, but the solvent pair ethanol/H_2O gave the best result in terms of yield and quality of crystals. The three compounds exhibit different topologies, induced by the different carboxylate ligands used.[30] The MOF compounds are insoluble in most organic solvents, except dimethyl sulfoxide and *N,N'*-dimethylformamide.

The combination Zn(II)/4,4'-bpy/formate generates an intricate 3D framework of **1**. The bridging of zinc(II) ions by formato ligands produces a 1D chain constituted of heptanuclear rings (Fig. 1A). The complete replacement of formate by acetate results in the formation of a 1D network (compound **2**; Fig. 1B). This simple framework is built from trinuclear acetato-bridged units that are linked to two adjacent ones, to form a three-leg ladder. The use of propionate as co-ligand yields a 2D network (Fig. 1C) which presents similarities with **2**. In fact, the framework of **3** contains the three-leg ladders observed in the solid-state structure of **2**. In **3**, these three-leg ladders are further connected to each other via 4,4'-bpy ligands.

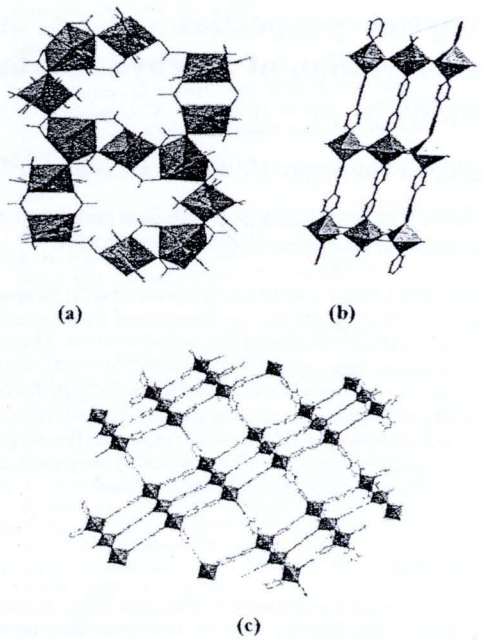

Fig. 1. (a) Perspective view of the 3D framework of **1**; (b) perspective view of the 1D three-leg ladder observed for **2** and; (c) perspective view of a 2D layer of **3**. The counter anions and the lattice water molecules have been omitted for clarity.

Zn(II) Compounds Doped with Cu(II) and Mn(II)

The three zinc(II) compounds were prepared in the presence of doping amounts of paramagnetic metal ions (Cu(II) and Mn(II)) to investigate the potential cation-exchange properties of MOFs with structure retention, and analyze the coordination geometry(ies) around the Zn(II) ions. The doped materials were prepared in ethanol/H_2O, using Zn(II)/Cu(II) and Zn(II)/Mn(II) ratios of 95:5, and in the presence of one equivalent of 4,4'-bpy ligand. All doped compounds have been characterized by XRPD, IR spectroscopy and EPR at RT and 70 K (see Figs. S1-S3). The IR spectra of the doped compounds are similar to that of the original Zn(II) compound, thus indicating that the structure and therefore the environment around the zinc(II) centers are not altered.

For instance, the polycrystalline EPR spectrum of the trinuclear Zn(II) compound **2** doped with Cu(II) shows signals revealing the presence of two different types of Cu(II) species. Each one is characterized by a four-lines hyperfine pattern with $g_{//} = 2.343$ and 2.275; (with $A_{//} = 124$ and 126; red and blue dots in Fig. 2a) $g_{\perp} = 2.094$ and 2.094 in agreement with a distorted-octahedral geometry.[31] No super-hyperfine splitting is resolved. These EPR data are clearly indicative of the occurrence of two different environments for the Zn(II) ions in **2**, which have been replaced by Cu(II) ions. Actually, a close observation of the molecular structure of **2** clearly reveals the presence of two distinct coordination geometries for the zinc ions, a highly distorted octahedron (site I in Fig. 2b) and a perfect octahedron (site II in Fig. 2b).[13]. Each trinuclear zinc unit in **2** is formed by two external sites I and one central site II. The doping with Mn(II) ions leads to a heteronuclear compound, whose EPR spectrum shows only one set of six lines, characterizing a Mn(II)

CREATED USING THE RSC ARTICLE TEMPLATE (VER. 3.0) - SEE WWW.RSC.ORG/ELECTRONICFILES FOR DETAILS

ARTICLE TYPE

www.rsc.org/xxxxxx | XXXXXXXX

species (Fig. 3a). These data suggest that only one from the two potential coordination sites has experienced ion exchange. Most likely Mn(II) ions are only capable of occupying site II (Fig. 3b), since Mn(II) has the tendency to form regular octahedral complexes. The polycrystalline EPR spectra of **1** and **3** doped with Cu(II) and Mn(II) exhibit similar features, thus suggesting comparable ion-exchange properties (Fig. S1).

The influence of the nature of the doping metal ion, namely Cu(II) and Mn(II), has been successfully investigated by EPR. This study illustrates the flexibility of the coordination geometry of Cu(II) compared to Mn(II). Such investigations are of great interest in the context of potential cation-exchange properties of MOFs with structure retention.

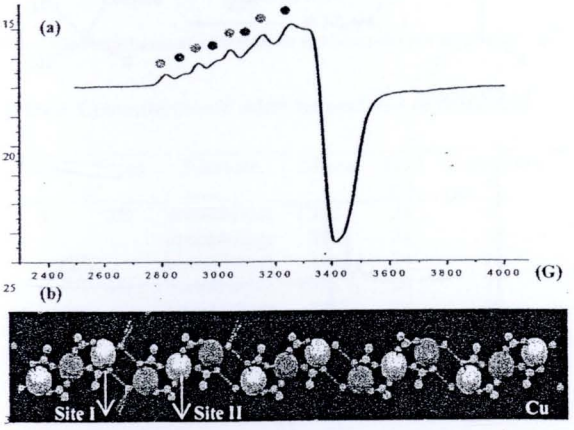

Fig. 2. (a) Polycrystalline EPR spectrum of **2** doped with Cu(II), recorded at 70 K. The two species are illustrated by blue and red dots. (b) Trinuclear Zn(II) units of **2** where zinc(II) ions (pink) have been replaced by Cu(II) ions (green) in two different sites (sites I and II).

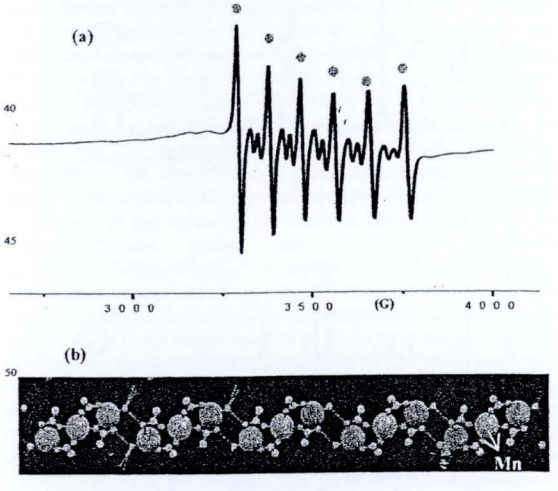

Fig. 3. (a) Polycrystalline EPR spectrum of **2** doped with Mn(II), recorded at 70 K and (b) trinuclear Zn(II) unit of **2** where only the central Zn(II) sites have been replaced by Mn(II) ions.

Removal and Reintroduction of Guest Molecules

The single-crystal X-ray structures of **1-3** reveal the presence of lattice water molecules, indicating a potential porosity of the materials. Thus, all three room-temperature stable compounds exhibit open channels that are occupied by guest water molecules. The possibility of generating microporous frameworks by removing the guest molecules has therefore been investigated. Hence, the stability of the different frameworks upon removal/reintroduction of the guest molecules has been monitored in detail, using TGA and XRPD techniques.

In the TGA curves of all compounds,[39] the first weight loss of 5.50% for **1**, 5.82% for **2** and 3.50% for **3** in the temperature range 71-201 °C, corresponds to the loss of the coordinated waters and guest water molecules. The loss of the coordinated aqua ligands is not observed below about 180 °C, apparently as the result of their strong coordination to the Zn(II) centers. Upon evacuation at 140 °C for 8 h under reduced pressure, compounds **2** and **3** experience weight losses consistent with the removal of all water molecules, behaving as second generation porous coordination polymers which have rigid vacant channels formed after the removal of guest molecules (Scheme 1) as is clear from the main peaks of XRPD patterns.[32] While the weight losses of compound **1** consist of all water molecules and four formate groups when elevating the temperature to 140 °C for 8 h under vacuum, the loss four formate groups does affect the framework skeleton. X-ray power diffraction reveals the structure change, but this compound remains a microcrystalline solid, as evidence by XRPD pattern (Fig. 4A) according to the result of the elemental analysis and corresponds to the formula of $Zn(4,4'\text{-bpy})_{2.5}(ClO_4)_2$, calcd.: C 45.86, H 3.07, N 10.70: found: C 44.67, H 3.01, N 10.56. (Table 1). So, the zinc(II)-formate compound **1** containing **4,4'-bpy** organic ligand is unstable at high temperature. On the other hand after removal of the guest molecules from crystalline **3**, the XRPD pattern of the resulting material **3c** is almost identical to the theoretical one of starting material **3** (Fig. 4C). These data clearly suggest that **3c** exhibits the original structure of **3** with empty channels. This behavior is also observed for compound **2** (Fig. 4B), therefore indicating that the solid-state structures of **2** and **3** do not collapse when the water molecules are taken out. Interestingly, the guest water species can be reintroduced into the evacuated samples of the three compounds by simple immersion in water for 48 h, as confirmed by XRPD measurements (Fig. 4), and elemental analyses (Table 1). In case of compound **1**, the elemental analysis data after reintroduction of water indicates the formula to be $Zn(4,4'\text{-bpy})_2(H_2O)(ClO_4)_2$, calcd.: C 40.39, H 3.05, N 9.42: found: C 41.43, H 3.50, N 8.96 (Table 1). Thus, after removal of the water/formate molecules, the microporous solids $Zn(4,4'\text{-bpy})_{2.5}(ClO_4)_2$ (**1c**), $\{Zn_3(4,4'\text{-bpy})_3(\mu\text{-}O_2CCH_3)_4(PF_6)_2\}_n$ (**2c**) and $\{Zn_3(4,4'\text{-bpy})_4(\mu\text{-}O_2CCH_2CH_3)_4(ClO_4)_2(4,4'\text{-bpy})_2\}_n$ (**3c**)

Table 1 Elemental analyses of compounds **1-3** and of the products after removal and after reintroduction of the guest water molecules.

Compound	Element	Exp.	Cal.	After Removal of water		After water Reintroduction (Exp.)
				Exp.	Cal.	
1	C	39.22	39.23	44.67	41.76	41.43
	H	3.31	3.37	3.01	2.88	3.50
	N	8.22	8.21	10.56	8.74	8.96
2	C	36.41	36.40	38.68	38.33	37.04
	H	3.23	3.33	2.80	3.50	3.16
	N	6.30	6.70	7.81	7.06	7.09
3	C	51.19	50.97	53.19	53.23	49.30
	H	4.84	4.51	4.09	4.22	3.93
	N	9.91	9.91	10.36	10.35	9.51

CREATED USING THE RSC ARTICLE TEMPLATE (VER. 3.0) - SEE WWW.RSC.ORG/ELECTRONICFILES FOR DETAILS

ARTICLE TYPE www.rsc.org/xxxxxx | XXXXXXXX

Scheme 1

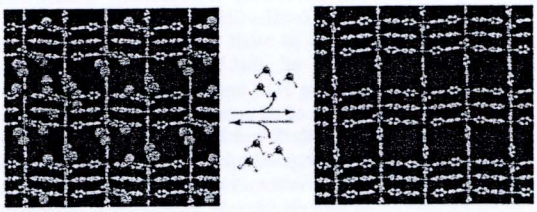

are generated with retention of the original frameworks (of compounds **2** and **3**). Such microporous materials with high-thermal stabilities and host-guest properties are relatively rare and have therefore great potential for practical applications.

Catalytic properties

Porous MOFs **1-3** have been tested as heterogeneous catalysts for the cyanosilylation of acetaldehyde and benzaldehyde. Thus, the selectivity and activity of the 3D (**1**), 1D (**2**) and 2D (**3**) coordination polymers have been examined. Typically, the powdered catalyst (**1-3**) is suspended in dichloromethane (CH_2Cl_2) or tetrahydrofuran (THF). The aldehydic substrate and trimethylsilyl cyanide (1:2 molar ratio) are subsequently added at room temperature and the reaction is carried out for 24 h (Scheme 2).[27, 29] The course of the reactions has been monitored by gas chromatography (GC).

Blank reactions have been performed by carrying the cyanosilylation of acetaldehyde and benzaldehyde without catalyst, at 25 °C. These test reactions give only conversions of 18% for acetaldehyde and 10% for benzaldehyde, after a reaction time of 24 h. When 40 mg of solid **1** is used as catalyst, a conversion of 95% of acetaldehyde is reached after 24 h reaction time in CH_2Cl_2 (Table 3 and Fig. 5). This high conversion suggests first that **1** acts as a very efficient catalyst for this reaction, and that both acetaldehyde and trimethylsilyl cyanide can diffuse swiftly through the pores to attain the Lewis metallic sites, to generate 2-(methylsiloxy)propioonitrile with a yield of 95% (71% when using **2** and 86% with **3**).

When benzaldehyde, a sterically more demanding substrate, is used under similar reaction conditions, a conversion of only 22% is observed (21% for **2** and 22% for **3**; Table 3). This significantly lower reactivity suggests that the dimension of the channels of the MOF plays an important role and leads to size selectivity.

Next, the influence of another organic solvent, namely THF, on the conversion of acetaldehyde has been examined for each MOF catalyst. It has been found that the reaction is less efficient in THF, which may be explained by a competitive binding of the substrate and the solvent to the metal site. This competitive binding obviously does not occur with CH_2Cl_2.

For instance, in THF, compound **1** promotes the conversion of only 38% acetaldehyde (30% for **2** and 57% for **3**; Table 3). The cationic nature and Lewis acidity of the Zn^{2+} center may play a role and lead to significantly different in the conversion (Fig. 6).

In contrast to the reactions performed in CH_2Cl_2, **3** is more efficient than **1** in THF (Table 3). These disparities regarding the distinct catalytic activities in CH_2Cl_2 and THF may be explained by structural features characterizing both compounds. As reported earlier,[13] the 3D framework of **1** exhibits channels filled by disordered perchlorate anions. The crystal packing of the 2D framework of **3** generates huge cavities filled with non-coordinated 4,4'-bipyridine (**4,4'-bpy**) molecules. Most likely, the slightly more polar solvent THF is capable of displacing the **4,4'bpy** guest molecules of **3** (which is obviously not the case with CH_2Cl_2), therefore increasing the accessibility of the aldehydic substrate to the metal centers.

The catalytic activities of compounds **1-3** for the cyanosilylation of aldehydes have been compared with those of other porous coordination frameworks. Fujita and co-workers reported the first coordination polymeric catalyst, *i.e.* {Cd(4,4'-

Scheme 2

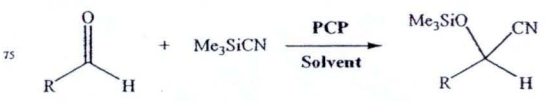

R= CH_3, phenyl

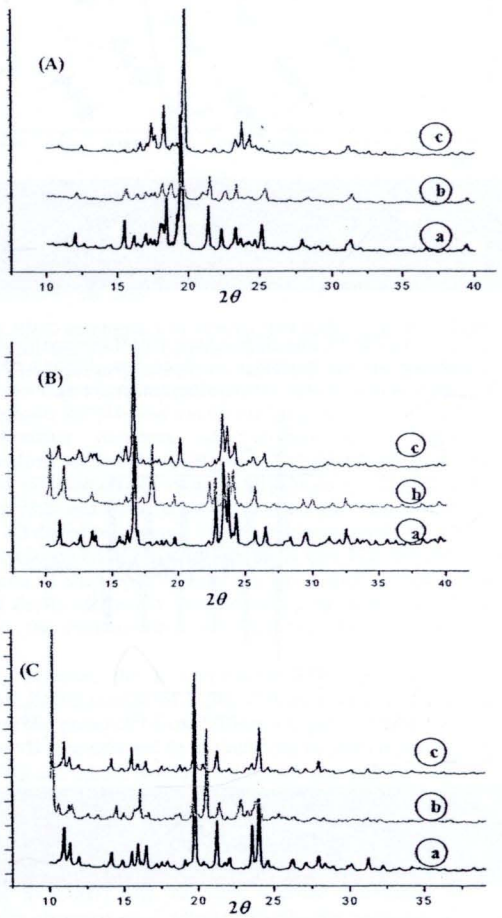

Fig. 4. (A) XRPD patterns of (a) **1** as-synthesized, (b) after removal of the guest water molecules, and (c) after reintroduction of the guest water molecules. (B) XRPD patterns of (a) **2** as-synthesized, (b) after removal of the guest water molecules, and (c) after reintroduction of the guest water molecules. (C) XRPD patterns of (a) **3** as-synthesized, (b) after removal of the guest water molecules, and (c) after reintroduction of the guest water molecules.

CREATED USING THE RSC ARTICLE TEMPLATE (VER. 3.0) - SEE WWW.RSC.ORG/ELECTRONICFILES FOR DETAILS

ARTICLE TYPE

www.rsc.org/xxxxxx | XXXXXXXX

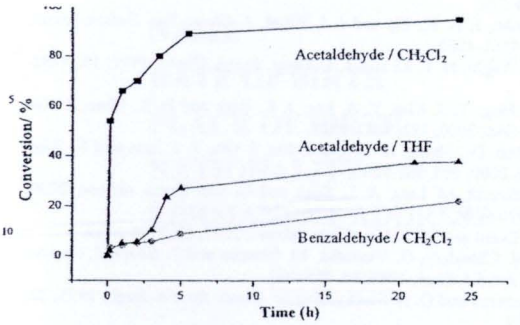

Fig. 5. Cyanosilylation of acetaldehyde and benzaldehyde with MOF **1** as catalyst

Table 3. Cyanosilylation of aldehydes catalyzed by compounds **1-3**.

Catalyst	Types	Substrate	Solvent	Time (h)	Conversion %
1	3D	acetaldehyde	CH_2Cl_2	24	95
		acetaldehyde	THF	24	38
		benzaldehyde	CH_2Cl_2	24	22
2	1D	acetaldehyde	CH_2Cl_2	24	71
		acetaldehyde	THF	24	30
		benzaldehyde	CH_2Cl_2	24	21
3	2D	acetaldehyde	CH_2Cl_2	24	86
		acetaldehyde	THF	24	57
		benzaldehyde	CH_2Cl_2	24	22

bpy)$_2$(NO$_3$)$_2$}$_n$,[23] for the cyanosilylation of aldehydes. This square network material is highly shape-selective, which is illustrated by the inclusion of *ortho*-dihalogenobenzenes, whereas the *meta*- and *para*-isomers do not form clathrates. Shape specificity has been observed as well with this compound for the cyanosilylation of aldehydes. For example, the conversion of 2-tolualdehyde (40%) is significantly higher than that of 3-tolualdehyde (19%). In addition, α- and β-naphthaldehydes' are good substrates in which can be converted with yields of 62% and 84%, respectively. The more sterically-demanding 9-anthraldehyde is hardly cyanosilylated. These shape specificities may be ascribed to the size of the cavity of the network material. In 2004, the same research group has synthesized {Cd(4,4'-bpy)$_2$(H$_2$O)$_2$(NO$_3$)$_2$·4H$_2$O}$_n$,[33] a square network to investigate mechanistic aspects of this cyanosilylation reaction. Thus, the catalytic study has been extended to the cyanosilylation of imines to gain some mechanistic insights in the heterogeneous catalysis mediated by the coordination compound. It has been found that the substrate accommodated in the square cavity, can easily coordinate to the Cd^{2+} center of the next network layer. It has therefore been suggested that the active sites exist mainly around the surface of the solid. They noted that, given a surface-promoted reaction, the catalytic activity of this porous polymer is remarkably high. Moreover, the Cd(II) center is more cationic and stronger Lewis acidic than mononuclear Cd(NO$_3$)$_2$·4H$_2$O. Size-selective reactions involving a MOF catalyst have been recently reported for Mn$_3$[(Mn$_4$Cl)$_3$(BTT)$_8$(CH$_3$OH)$_{10}$]$_2$ (H$_3$BTT=1,3,5-benzenetris tetrazol-5-yl),[29] wherein Mn^{2+} ions exposed on the surface of the framework might serve as potential Lewis acidic sites. Indeed, this MOF catalyzes the cyanosilylation of aromatic aldehydes and ketones, as well as the Mukaiyama-aldol reaction. In each case, a pronounced size-selectivity effect consistent with the pore dimensions is observed.

Heterogeneity

The heterogeneity of the catalytic reaction has been probed for the cyanosilylation of acetaldehyde in THF, mediated by compound **1**. Thus, the catalyst (compound **1**) has been filtered out after a reaction time of 5 h, corresponding to an acetaldehyde conversion of 24% (Fig. 7). The filtrate has been stirred for 24 h and no further conversion of the substrate is observed (about 25% conversion; Fig. 7). This result clearly demonstrates that no homogeneous catalytic species is present in solution. Next, the filtrate has been divided into two equal parts. The first part has been stirred with fresh catalyst **1** while the other one has been stirred without catalyst. In the filtrate without catalyst, the reaction does not proceed further, whereas in the catalyst-containing suspension, the conversion of the substrate is

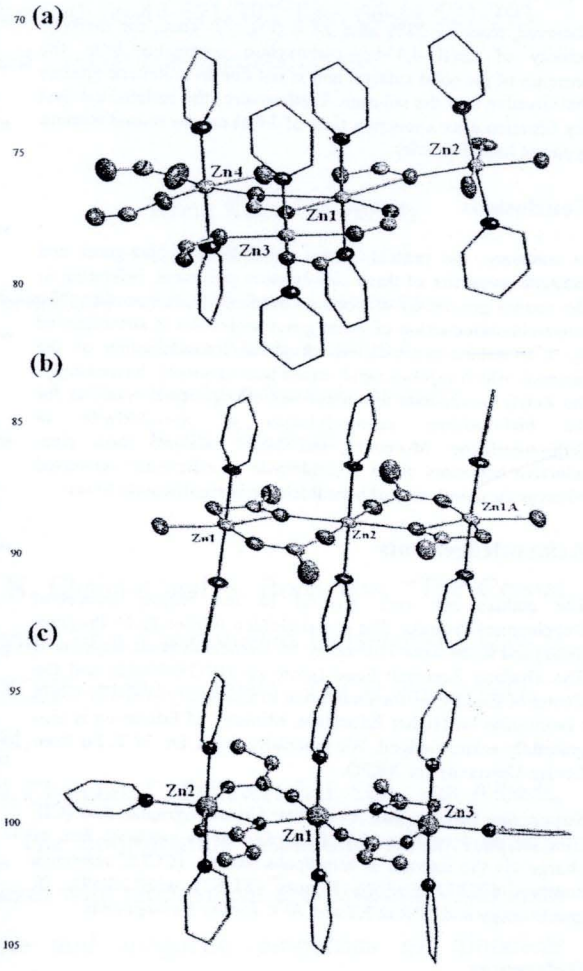

Fig. 6. Representation of the asymmetric units of (a): **1**, (b): **2** and (c): **3**, showing the atom-labeling schemes for the zinc(II) ions. The perchlorate anions and the lattice water molecules are not shown for clarity.

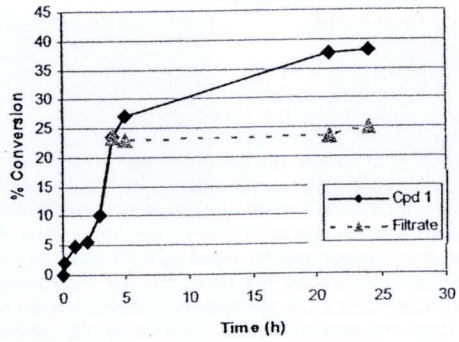

Fig. 7. Cyanosilylation of acetaldehyde in THF catalysed by **1**

observed, reaching 38% after 24 h (Fig. 7). Thus, the catalytic activity of Zn(II)-4,4'-bpy-carboxylato originates from the presence of the solid catalyst and is not due to molecular species that dissolve into the solution. Furthermore, the isolated catalyst (by filtration after a reaction time of 24 h) can be reused without apparent loss of activity.

Conclusions

In summary, the present study, describes the host-guest and catalytic properties of three coordination polymers, belonging to the second generation of porous coordination compounds. The removal/reintroduction of water guest molecules is accompanied by a crystalline-to-crystalline structural transformation of the material, which exhibits rigid vacant host channels. Interestingly, the Zn(II) compounds are effective heterogeneous catalysts for the high-yielding cyanosilylation of acetaldehyde in dichloromethane. Moreover, the MOF catalysts show size-selective behaviors since acetaldehyde is efficiently converted whereas the conversion of benzaldehyde is significantly lower.

Acknowledgements

The authors are very grateful to the Higher Education Development Projects: The Royal Golden Jubilee Ph.D. Program (RGJ) and Khon Kean University for a research grant. Support of The Thailand Research Fund (grant no BRG5280012) and the Center of Excellence for Innovation in Chemistry (PERCH-CIC), Commission on Higher Education, Ministry of Education is also gratefully acknowledged. We gratefully thank Dr. W.T. Fu from Leiden University for XRPD.

Supporting Information Available: Crystallographic data (CIF files for the 3 compounds). This material is available free of charge via the internet at http://pubs.acs.org, (CCDC reference numbers 699370–699372). Figures (S1-S3) with XRPD, IR spectroscopy and EPR at RT and 70 K for the 3 compounds.

References

1. H. J. Choi and M. P. Suh, *J. Am. Chem. Soc.*, 2004, **126**, 15844-15851.
2. J. W. Ko, K. S. Min and M. P. Suh, *Inorg. Chem.*, 2002, **41**, 2151-2157.
3. M. P. Suh, H. J. Choi, S. M. So and B. M. Kim, *Inorg. Chem.*, 2003, **42**, 676-678.
4. S. Muthu, J. H. K. Yip and J. J. Vittal, *J. Chem. Soc. Dalton Trans.*, 2002, 4561-4568.
5. O. M. Yaghi, H. L. Li and T. L. Groy, *Inorg. Chem.*, 1997, **36**, 4292-4293.
6. O. S. Jung, Y. J. Kim, Y. A. Lee, J. K. Park and H. K. Chae, *J. Am. Chem. Soc.*, 2000, **122**, 9921-9925.
7. J. S. Seo, D. Whang, H. Lee, S. I. Jun, J. Oh, Y. J. Jeon and K. Kim, *Nature*, 2000, **404**, 982-986.
8. M. Albrecht, M. Lutz, A. L. Spek and G. van Koten, *Nature*, 2000, **406**, 970-974.
9. O. R. Evans and W. B. Lin, *Chem. Mater.*, 2001, **13**, 2705-2712.
10. B. M. Choudary, G. Vasantha, M. Sharma and P. Bharathi, *Angew. Chem. Int. Ed. Engl.*, 1989, **28**, 465-466.
11. P. Behrens and G. D. Stucky, *Angew. Chem. Int. Ed. Engl.*, 1993, **32**, 696-699.
12. V. Ramamurthy and D. R. Sanderson, *Tetrahedron Lett.*, 1992, **33**, 2757-2760.
13. J. M. Thomas, *Angew. Chem. Int. Ed. Engl.*, 1988, **27**, 1673-1691.
14. S. L. Suib, *Chem. Rev.* 1993, **93**, 803-826.
15. V. L. K. Valli and H. Alper, *J. Am. Chem. Soc.*, 1993, **115**, 3778-3779.
16. D. N. Dybtsev, A. L. Nuzhdin, H. Chun, K. P. Bryliakov, E. P. Talsi, V. P. Fedin and K. Kim, *Angew. Chem. Int. Ed.*, 2006, **45**, 916-920.
17. C. D. Wu, A. Hu, L. Zhang and W. B. Lin, *J. Am. Chem. Soc.*, 2005, **127**, 8940-8941.
18. S. H. Cho, B. Q. Ma, S. T. Nguyen, J. T. Hupp and T. E. Albrecht-Schmitt, *Chem. Commun.*, 2006, 2563-2565.
19. P. Horcajada, S. Surble, C. Serre, D. Y. Hong, Y. K. Seo, J. S. Chang, J. M. Greneche, I. Margiolaki and G. Ferey, *Chem. Commun.*, 2007, 2820-2822.
20. S. Hasegawa, S. Horike, R. Matsuda, S. Furukawa, K. Mochizuki, Y. Kinoshita and S. Kitagawa, *J. Am. Chem. Soc.*, 2007, **129**, 2607-2614.
21. O. R. Evans, H. L. Ngo and W. B. Lin, *J. Am. Chem. Soc.*, 2001, **123**, 10395-10396.
22. K. Schlichte, T. Kratzke and S. Kaskel, *Micropor. Mesopor. Mater.*, 2004, **73**, 81-88.
23. M. Fujita, Y. J. Kwon, S. Washizu and K. Ogura, *J. Am. Chem. Soc.*, 1994, **116**, 1151-1152.
24. L. Meia, S.-W. Longa, H.-K. Liang and W.-S. Xuana, *Appl. Organometal. Chem.*, 2008, **22**, 181.
25. Z. Zeng, G. Zhao and Z. Zhou, C. Tang, *Eur. J. Org. Chem.*, 2008, 1615.
26. A. Henschel, K. Gedrich, R. Kraehnert and S. Kaskel, *Chem. Commun.*, 2008, 4192-4194.
27. M. Dinca, A. Dailly, Y. Liu, C. M. Brown, D. A. Neumann and J. R. Long, *J. Am. Chem. Soc.*, 2006, **128**, 16876-16883.
28. S. T. Kadam and S. S. Kim, *Appl. Organometal. Chem.*, 2009, **23**, 119-123.
29. S. Horike, M. Dinca, K. Tamaki and J. R. Long, *J. Am. Chem. Soc.*, 2008, **130**, 5854-+.
30. P. Phuengphai, S. Youngme, P. Kongsaeree, C. Pakawatchai, N. Chaichit, S. J. Teat, P. Gamez and J. Reedijk, *Crystengcomm*, 2009, **11**, 1723-1732.
31. B. J. Hathaway, G. Wilkinson, R. D. Gill and J. A. McCleverty, *Comprehensive Coordination Chemistry*, 1987, (Eds.) 5, Pergamon Press, Oxford,.
32. S. Noro, R. Kitaura, M. Kondo, S. Kitagawa, T. Ishii, H. Matsuzaka and M. Yamashita, *J. Am. Chem. Soc.*, 2002, **124**, 2568-2583.
33. O. Ohmori and M. Fujita, *Chem. Commun.*, 2004, 1586-1587.

CURRICULUM VITAE

NAME	MR. PONGTHIPUN PHUENGPHAI
DATE OF BIRTH	MAY 25th, 1978
PLACE OF BIRTH	SURIN, THAILAND
NATIONALITY	THAI
PERMANENT ADDRESS	CHEMISTRY PROGRAM SCIENCE AND TECHNOLOGY FACULTY SURINDRA RAJHABHAT UNIVERSITY SURIN 32000 THAILAND Office: Tel. 66-44-521-393 Fax. 66-44-521-393 E-mail : pongtipun@hotmail.com

EDUCATION

2009	Ph.D (Chemistry)	Khon Kaen University Khon Kaen, Thailand
2004	M.Sc (Inorganic Chemistry)	Khon Kaen University Khon Kaen, Thailand
2000	B.Ed (Chemistry)	Rajabhat Surin University Surin, Thailand

RESEARCH PUBLICATIONS

(1) S. Youngme, **P. Phuengphai**, N. Chaichit and S. Booncoon, "The Crystal Structure and Electronic Properties of a Cis-distorted Octahedral CuN4O2 Chromophore: $[Cu(dpyam)_2(OXO)]^+$, OXO = ONO^-, O_2CH and ONO_2^-", *Polyhedron*, 2004, 23, 1685-1694.

(2) S. Youngme, **P. Phuengphai**, N. Chaichit, C. Pakawatchai, G.A. van Albada, O. Roubeau, and J. Reedijk, "The coordination chemistry of mono(di-2-pyridylamine) copper(II) complexes with monovalent and divalent oxoanions: Crystal structure, spectroscopic and magnetic properties of dinuclear $[Cu(L)(\mu\text{-}H_2PO_4)(H_2PO_4)]_2$ and polynuclear $[Cu(L)(\mu_3\text{-}HPO_4)]_n$", *Inorg. Chim. Acta*, 2004, 357, 3603-3612.

(3) S. Youngme, **P. Phuengphai**, N. Chaichit, G.A. van Albada, O. Roubeau and J. Reedijk "An unprecedented tetranuclear Cu(II) cluster, exclusively bridged by two μ_3,η^3-hydrogenphosphate anions. Synthesis, structure, and magnetic properties" *Inorg. Chim. Acta*, 2005, 358, 849-853.

(4) S. Youngme, **P. Phuengphai**, N. Chaichit, G.A. van Albada, O. Roubeau and J. Reedijk "A novel tetranuclear hydrogenphosphatebridged Cu(II) cluster. Synthesis, structure, spectroscopy and magnetism of $[Cu_4(dpyam)_4(\mu_4,\eta^3\text{-}HPO_4)_2(\mu\text{-}X)_2]X_2(H_2O)_6$ (X = Cl, Br)" *Inorg. Chim. Acta*, 2005, 358, 2262-2268.

(5) S. Youngme, **P. Phuengphai**, C. Pakawatchai, G.A. van Albada, S. Tanase, I. Mutikainen, U. Turpeinen and J. Reedijk "A copper(II) chain compound with hydrogenphosphate bridges organized in a double chain structure. Synthesis, structure and magnetic properties of $[Cu(1,10\text{-phenanthroline})(\mu\text{-}HPO_4)(H_2O)_2]_n$" *Inorg. Chem. Commun.*, 2005, 8, 335-338.

(6) S. Youngme, **P. Phuengphai**, C. Pakawatchai, G.A. van Albada and J. Reedijk "A novel polymeric trinuclear-based μ_3-phosphato-bridged Cu(II) complex containing two different types of monophosphate. Synthesis, structure and magnetism of $\{[Cu_3(di\text{-}2\text{-}pyridylamine)_3(\mu_3,\eta^3\text{-}HPO_4)(\mu_3,\eta^4\text{-}PO_4)(H_2O)][(PF_6)(H_2O)_3\}_n$" *Inorg. Chim. Acta*, 2005, 358, 2125-2128.

(7) S. Youngme, **P. Phuengphai**, N. Chaichit, G.A. van Albada, S. Tanase and J. Reedijk "Synthesis, crystal structure and magnetic properties of a polynuclear Cu(II) complex: catena-poly[aqua(di-2-pyridylamine)copper(II) (μ-formato-O,O')nitrate]" *Inorg. Chim. Acta*, 2005, 358, 3267-3271.

(8) **P. Phuengphai**, S. Youngme, C. Pakawatchai, G.A. van Albada, M. Quesada and J. Reedijk "Synthesis, crystal structure and magnetic properties of an unexpected new coordination Cu(II) compound, containing two different phosphato-bridged dinuclear units; $[Cu_2(phen)_2(\mu\text{-}H_2PO_4\text{-}O,O')_2(H_2PO_4)_2]$ $[Cu_2(phen)_2(\mu\text{-}H_2PO_4\text{-}O,O')(\mu\text{-}H_2PO_4\text{-}O)(\mu\text{-}HPO_4\text{-}O)]_2(H_2O)_9$ (phen = 1,10-phenanthroline)" *Inorg. Chem. Commun.*, 2006, 9, 147-151.

(9) **P. Phuengphai**, S. Youngme, N. Chaichit, C. Pakawatchai, G.A. van Albada, M. Quesada and J. Reedijk, "Crystal structures and magnetic properties of two new phosphate-metal complexes: $[Cu_2(bpy)_2(\mu,\eta^2\text{-}HPO_4)(\mu,\eta^1\text{-}H_2PO_4)(\mu,\eta^2\text{-}H_2PO_4)]_n$", *Polyhedron*, 2006, 25, 2198-2206.

(10) S. Youngme, **P. Phuengphai**, N. Chaichit, I. Mutikainen, U. Turpeinen and B. M. Murphy "Crystal structures and electronic properties of three fluxional [Cu(di-2-pyridylamine)$_2$(OXO)]Y complexes" *J. Coord. Chem.*, 2007, 60, 131-142.

(11) S. Youngme, **P. Phuengphai**, C. Pakawatchai, P. Kongsaeree, N. Chaichit, "Five-coordinate copper(II) complexes: crystal structures, spectroscopic properties and new extended structural pathways of [Cu(chelate)$_2$X]Y, where chelate = dpyam, phen and bipy; X =pseudohalide ligands" *ACTA CRYST. B.*, 2008, 64 , 318-329.

(12) **P. Phuengphai**, S. Youngme, P. Kongsaeree, C. Pakawatchai, N. Chaichit, S. J. Teat, P. Gamez and J. Reedijk, "Drastic steric effects from, respectively, a hydrogen, a methyl and an ethyl group on the coordination network of a zinc(II)–4,4'-bipyridine–carboxylato ternary system" *CrystEngComm.*, 2009, 11 , 1723-1732.

(13) **P. Phuengphai**, S. Youngme, P. Gamez and J. Reedijk, "Catalytic properties of a series of coordination networks: cyanosilylation of aldehydes catalyzed by Zn(II)-4,4'-bpy-carboxylato complexes" *Dalton Trans.* (2010) accepted.